2017-06

Control system development for power generation from small-scale compressed air energy storage

Vranas, Todd M.

Monterey, California: Naval Postgraduate School

NAVAL POSTGRADUATE SCHOOL

MONTEREY, CALIFORNIA

THESIS

CONTROL SYSTEM DEVELOPMENT FOR POWER GENERATION FROM SMALL-SCALE COMPRESSED AIR ENERGY STORAGE

by

Todd M. Vranas

June 2017

Thesis Advisor: Anthony Gannon
Co-Advisor: Andrea Holmes

THIS PAGE INTENTIONALLY LEFT BLANK

REPORT DOCUMENTATION PAGE			Form Approved OMB No. 0704–0188
Public reporting burden for this collection of information is estimated to average 1 hour per response, including the time for reviewing instruction, searching existing data sources, gathering and maintaining the data needed, and completing and reviewing the collection of information. Send comments regarding this burden estimate or any other aspect of this collection of information, including suggestions for reducing this burden, to Washington headquarters Services, Directorate for Information Operations and Reports, 1215 Jefferson Davis Highway, Suite 1204, Arlington, VA 22202-4302, and to the Office of Management and Budget, Paperwork Reduction Project (0704-0188) Washington, DC 20503.			
1. AGENCY USE ONLY ***(Leave blank)***	**2. REPORT DATE** June 2017	**3. REPORT TYPE AND DATES COVERED** Master's thesis	
4. TITLE AND SUBTITLE CONTROL SYSTEM DEVELOPMENT FOR POWER GENERATION FROM SMALL-SCALE COMPRESSED AIR ENERGY STORAGE			**5. FUNDING NUMBERS**
6. AUTHOR(S) Todd M. Vranas			
7. PERFORMING ORGANIZATION NAME(S) AND ADDRESS(ES) Naval Postgraduate School Monterey, CA 93943-5000			**8. PERFORMING ORGANIZATION REPORT NUMBER**
9. SPONSORING /MONITORING AGENCY NAME(S) AND ADDRESS(ES) Office of Naval Research, Energy Systems Technology Evaluation Program (ESTEP), under the technical monitoring of Stacey Curtis, Marissa Brand and Richard Carlin			**10. SPONSORING / MONITORING AGENCY REPORT NUMBER**
11. SUPPLEMENTARY NOTES The views expressed in this thesis are those of the author and do not reflect the official policy or position of the Department of Defense or the U.S. Government. IRB number ____N/A____.			
12a. DISTRIBUTION / AVAILABILITY STATEMENT Approved for public release. Distribution is unlimited.			**12b. DISTRIBUTION CODE**

13. ABSTRACT (maximum 200 words)

This thesis is the development of an industrial control system to enable autonomous operation of the electrical generator for a small-scale compressed air energy storage system (SS-CAES).

The purpose of the SS-CAES is to facilitate electrical energy storage (EES) at Department of the Navy (DON) facilities using preexisting compressed air systems. Development of the control system focused on designing a robust control program that was scalable to enable application to a broad range of facilities. The control system accomplished scalability through a single control program by utilizing scalable commercial-off-the-shelf (COTS) hardware components.

The possible use of the SS-CAES for providing emergency electrical power requires the control system to be capable of a dark start. The term dark start refers to a power generation system that does not require electrical energy in the form of batteries or external power to begin operation. Dark start systems have the potential to store energy for extended periods of time without maintenance.

The implementation of this control system with retrofitted compressed air systems at DON facilities increases the viability of SS-CAES, enabling storage of electrical power produced by solar and wind generation.

14. SUBJECT TERMS compressed air, energy storage, small scale, electrical generation, supercapacitor, programmable logic controller, solenoid, relay, voltage transducer, dark start			**15. NUMBER OF PAGES** 103
			16. PRICE CODE
17. SECURITY CLASSIFICATION OF REPORT Unclassified	**18. SECURITY CLASSIFICATION OF THIS PAGE** Unclassified	**19. SECURITY CLASSIFICATION OF ABSTRACT** Unclassified	**20. LIMITATION OF ABSTRACT** UU

NSN 7540–01-280-5500 Standard Form 298 (Rev. 2–89)
Prescribed by ANSI Std. 239–18

THIS PAGE INTENTIONALLY LEFT BLANK

Approved for public release. Distribution is unlimited.

CONTROL SYSTEM DEVELOPMENT FOR POWER GENERATION FROM SMALL-SCALE COMPRESSED AIR ENERGY STORAGE

Todd M. Vranas
Lieutenant, United States Navy
B.S., Rensselaer Polytechnic Institute, 2010

Submitted in partial fulfillment of the
requirements for the degree of

MASTER OF SCIENCE IN MECHANICAL ENGINEERING

from the

NAVAL POSTGRADUATE SCHOOL
June 2017

Approved by: Anthony Gannon
Thesis Advisor

Andrea Holmes
Co-Advisor

Garth Hobson
Chair, Department of Mechanical and Aerospace Engineering

THIS PAGE INTENTIONALLY LEFT BLANK

ABSTRACT

This thesis is the development of an industrial control system to enable autonomous operation of the electrical generator for a small-scale compressed air energy storage system (SS-CAES).

The purpose of the SS-CAES is to facilitate electrical energy storage (EES) at Department of the Navy (DON) facilities using preexisting compressed air systems. Development of the control system focused on designing a robust control program that was scalable to enable application to a broad range of facilities. The control system accomplished scalability through a single control program by utilizing scalable commercial-off-the-shelf (COTS) hardware components.

The possible use of the SS-CAES for providing emergency electrical power requires the control system to be capable of a dark start. The term dark start refers to a power generation system that does not require electrical energy in the form of batteries or external power to begin operation. Dark start systems have the potential to store energy for extended periods of time without maintenance.

The implementation of this control system with retrofitted compressed air systems at DON facilities increases the viability of SS-CAES, enabling storage of electrical power produced by solar and wind generation.

THIS PAGE INTENTIONALLY LEFT BLANK

TABLE OF CONTENTS

LIST OF FIGURES

THIS PAGE INTENTIONALLY LEFT BLANK

LIST OF ACRONYMS AND ABBREVIATIONS

AC	alternating current
BESS	battery energy storage system
CAES	compressed air energy storage
DC	direct current
DON	Department of the Navy
EDLC	electric double layer capacitor
EES	electrical energy storage
FES	flywheel energy storage
GW	gigawatt(s)
HMI	human machine interface
IMPEL	integrated multi-physics energy lab
MW	megawatt(s)
NC	normally closed
NO	normally open
NPS	Naval Postgraduate School
NPT	national pipe thread
PHS	pumped hydroelectric storage
PLC	programmable logic controller
RES	renewable energy source
SECNAV	Secretary of the Navy
SMES	superconducting magnetic energy storage
SNG	synthetic natural gas
SS-CAES	small scale compressed air energy storage
SSR	solid state relay
TES	thermal energy storage
TWh	terawatt hour(s)
V	volts
W	watt(s)

THIS PAGE INTENTIONALLY LEFT BLANK

ACKNOWLEDGMENTS

I would like to thank my wife, Deana, for all her support. She manages all aspects of moves and household business, enabling me to focus more on my work. In addition, I appreciate all the hours she has spent proofreading this thesis along with my other academic work.

I would like to thank Josh Williams for all his assistance while at Naval Postgraduate School.

Finally, I would like to thank my advisors, Dr. Gannon and Ms. Holmes, for their advice and guidance in the development of this thesis.

THIS PAGE INTENTIONALLY LEFT BLANK

I. INTRODUCTION

A. NAVY ENERGY GOALS

The Secretary of the Navy (SECNAV) has established five energy goals, is shown in Figure 1. The focus of the goals is to create a Department of the Navy (DON) controlled energy infrastructure, providing energy security and independence [1]. Four of the energy goals specify reducing petroleum consumption, requiring the use of sustainable energy resources.

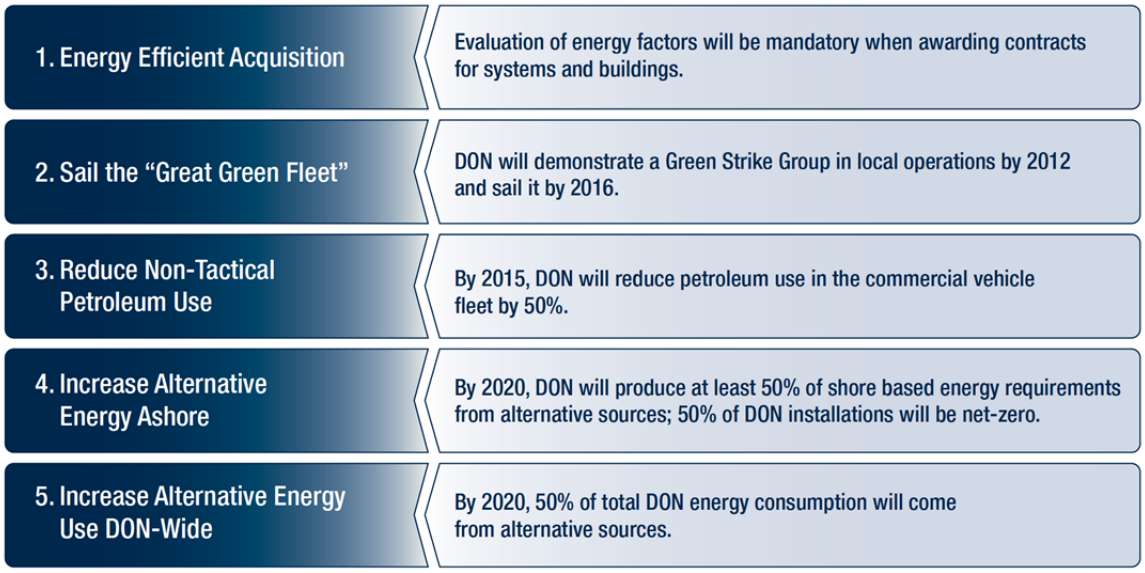

Figure 1 The Secretary of the Navy's Energy Goals. Source: [1].

The use of renewable energy resources enhances the tactical stance of the DON facilities and assets with a secondary benefit of being environmentally responsible. To foster energy security, the DON must become less reliant on petroleum and external electrical power. Offsite-produced petroleum and external electrical power requires transport to DON installations. The production facilities and transportation lines are vulnerabilities to the energy security of the DON. As stated by the Assistant Secretary of the Navy for Energy, Installations and Environment "The U.S. power grid relies heavily on technology dating back to the '60s and '70s. This aging infrastructure is vulnerable to

physical and cyber-attacks, natural disasters and malfunctions" [2]. There were 114 utility power outages lasting over eight hours at military installations in fiscal year 2014 [3]. Establishment of microgrids enables the use of sustainable energy sources, such as solar and wind. Decentralizing energy production in the form of microgrids on DON installations would enable more effective security and control [4].

In order to establish energy independence microgrids, DON installations must be able to supply enough power to meet requirements with no interruptions. Meaning, when demand is high or output is low something needs to compensate to maintain the grid. Many microgrids make use of fossil fuel-powered generators or power generated offsite [5]. The Navy has "1 gigawatt [of renewable power production] in final negotiations and under construction" but almost no storage capabilities [2]. The DON announced procurement of an 18 megawatt-hour (MWh) vanadium flow battery that will store electrical energy produce by solar to be installed at Naval Base Ventura County [6]. This flow battery is the first grid-level electrical energy storage system installed by the Navy. To become energy independent, the DON needs microgrids that include sufficient energy storage capabilities to meet demand.

B. THE SUSTAINABLE ENERGY PROBLEM

There exists an inherent problem with sustainable electrical generation, compared to conventional generation. Sustainable energy generation does not have a persistent reliable energy source that is controllably variable, which creates a significant obstacle to purely sustainable power grids. However, conventional fossil fuel powered generator sources can be brought online, taken offline, or throttle to match the load requirements of the grid [7].

Typical sustainable electrical generation sources include solar, wind, and marine, none of which is present continuously with a consistent magnitude. The most abundant of the sustainable energy resources is solar. Solar power is capable of producing 2830 times the global daily energy requirement [8]. The relative abundance of sustainable resources is shown in Figure 2.

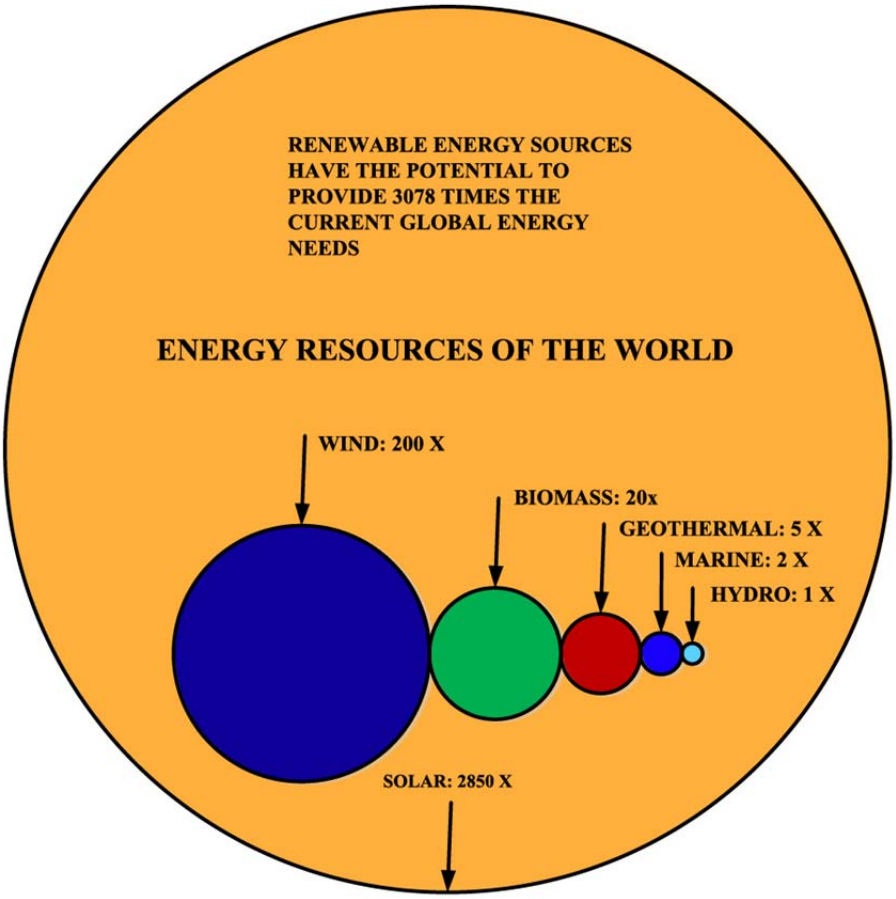

Figure 2 Abundance of Sustainable Energy Resources Based on Daily Global Demand. Source: [9].

The inconsistent nature of sustainable energy resources creates a significant problem for power production and quality. For example, despite knowing the period of solar radiation exposure on a solar panel the power output from the panel is not certain. The magnitude of the solar radiation received by the panel is dependent on prevailing conditions. Cloud cover significantly reduces the strength of solar radiation. In addition, the amount of dust covering the panel, as result of air pollution, also has a dramatic effect [10], [11]. However, even on the clearest day, with clean panels, the issue of persistence of the solar radiation remains. Electrical generators using solar radiation as an energy source will not produce electricity when not exposed to solar radiation; therefore solar generation is limited to the period post sunrise and pre sunset. Meaning, solar generators

may create all the electrical power required during the day but none at night. Similar issues exist with all other sustainable energy sources [12], [13].

Most current power grids utilizing sustainable generation sources mitigate the reliability issue by supplementing the power grid with fossil fuel-powered generators. These generators are also used to maintain the appropriate frequency of the electricity provided by the power grid, which is more easily done with a controllable generation source [14]. Using numerous types of sustainable resources reduces the amount of fossil fuel supplementation required. Suppose a power grid operated on purely solar during the day. At night, operation of fossil fuel-powered generators would be required to meet demand. If generators utilizing wind as a resource were added to the system, on nights when sufficient wind was present to meet the demand, operation of fossil fuel-powered generators would not be necessary. The more likely scenario would be a portion of the electricity generated at night would come from the generators utilizing wind and another portion from the fossil fuel-powered generators. While on nights with no wind, the fossil fuel generators would need to produce all of the electrical power required. Meaning fossil fuel-powered generators cannot be eliminated from power girds without robust and sufficient energy storage [15].

C. ENERGY STORAGE METHODS

To bridge the gap from unreliable sustainable resources to a reliable sustainable electrical power grid an electrical energy storage method is essential. There are many proposed options for electrical energy storage (EES) for a surplus of sustainable resources to be stored and then used when there is a deficit of sustainable resources [15–18]. While conditions for EES remain consistent, the type of energy storage varies widely. The various EES methods utilized are grouped into specific categories: mechanical, electrochemical, chemical, electrical, and thermal [16]. A breakdown of the various forms of EES is shown in Figure 3. Each energy storage state has distinct advantages and disadvantages.

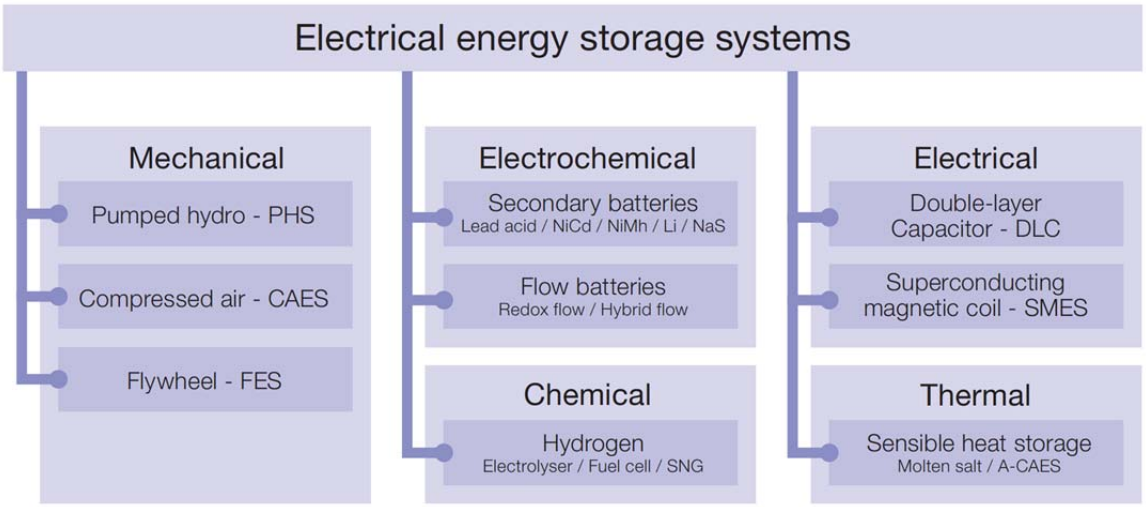

Figure 3 Electrical Energy Storage Systems Classified by Energy. Source: [16].

1. Pumped Hydroelectric Storage

Mechanical storage of electrical energy produced is the most prevalent EES method used [15]. A great majority of mechanical storage is in the form of pumped hydroelectric storage (PHS). PHS operates in a similar manner to a hydroelectric dam but with the capability to pump water back up to the top of the dam. Typical PHS plants consist of two reservoirs, one separated by vertical elevation linked by pipes and turbines attached to generators. A generic PHS plant is shown in Figure 4. Due to its relative simplicity and larger potential power outputs, compared to other EES systems, it has become a very popular EES method, accounting for over 100 GW worldwide [15]. The power output for modern PHS ranges from 100 MW to 3000 MW, which far exceeds the power output possible for most other EES [15].

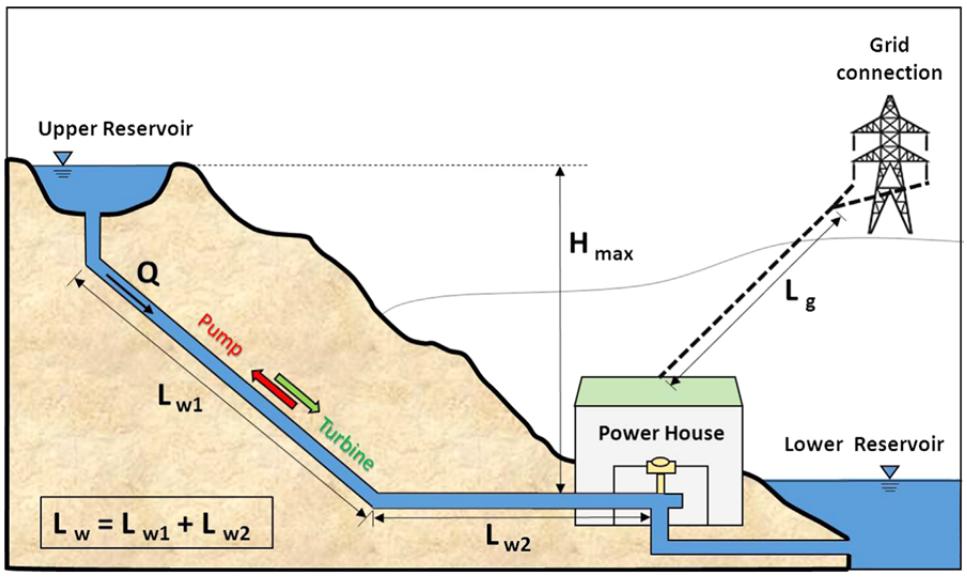

Figure 4 General Pumped Hydroelectric Storage Plant. Source: [19].

Despite its advantages, a few significant issues hold back PHS from being the complete solution to the world's energy storage needs. The most significant of which is the requirement of a substantial elevation difference between reservoirs, which is a determining factor for the power output of the plant [15], [19]. The large reservoirs also require vast areas of land that have an adequate geologic make up [17–19]. Thus, implementation of PHS is limited to areas with adequate topographic and geologic conditions.

2. Compressed Air Energy Storage

Compressed air energy storage (CAES) is the only energy storage method that approaches the power output of PHS. A single CAES unit is capable of putting out over 100 MW [15]. CAES plants are able to achieve this high power output by heating the stored compressed air before passing it over turbines. In mature designs, the heat source used is a non-renewable fossil fuel such as natural gas; such a non-adiabatic CAES plant is shown in Figure 5 [15–18]. The use of non-renewables makes commercially mature non-adiabatic designs for CAES undesirable option for a completely sustainable power system.

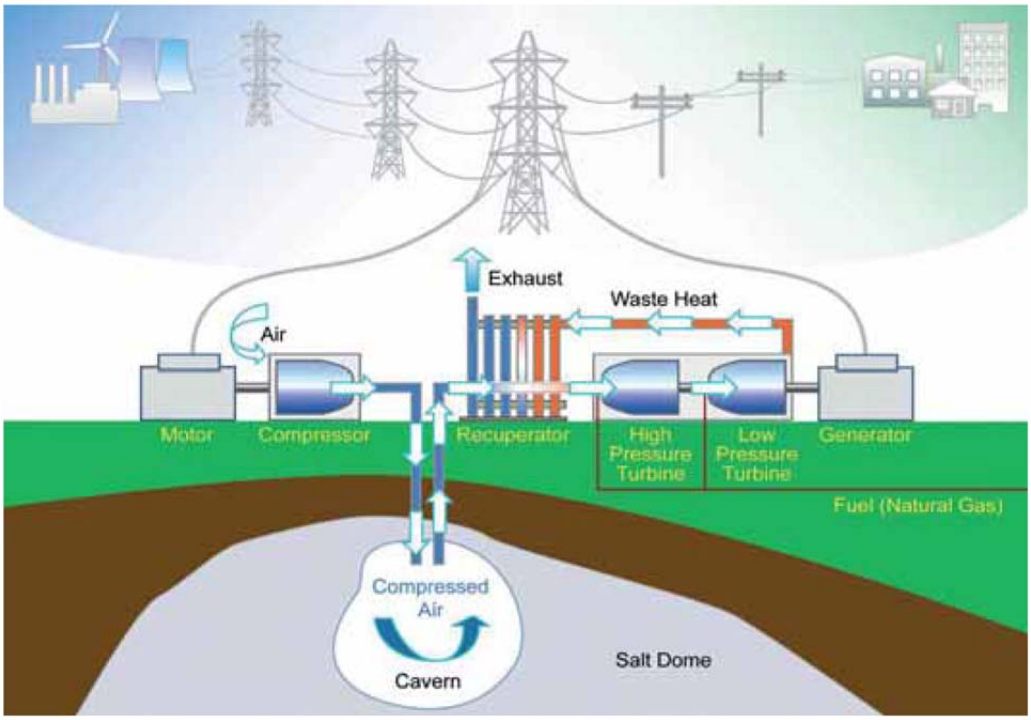

Figure 5 Non-adiabatic Compressed Air Energy Storage Plant. Source: [16].

In effort to create a sustainable CAES plant, adiabatic versions are in development [16], [17]. Designs for adiabatic CAES plants combine mechanical and thermal storage methods. Heat produced during the compression of the air is stored with a thermal storage method. Then, when the plant is to produce electrical power, the compressed air receives heat from the stored thermal energy rather than non-renewable fuels [16], [17]. Despite eliminating the use of fossil fuels, the adiabatic CAES designs in development are theoretically capable of producing similar power outputs to current non-adiabatic designs [16]. Therefore, adiabatic CAES are a viable sustainable EES option.

Both non-adiabatic and adiabatic CAES systems present significant impediments to a large-scale commercial adoption for EES; the most significant of these is geologic. CAES requires large compressed air storage caverns. Currently, there are only two commercial CAES plants worldwide, and both make use of large underground caverns created in previously mined salt domes [15]. Similar to the geologic constraints for PHS reservoirs, the CAES caverns must also have appropriate geology.

The geologic limitation to large-scale CAES systems has led to the development of smaller scale CAES systems for use in micro-grids and integrated power systems. These smaller scale systems make use of tanks and underwater bladders [20]. CAES that use tanks or caverns have a constant volume for storage, so the pressure available to the turbines is variable. Underwater bladders are unique storage methods because the working fluid remains at constant pressure. The bladder is able to change volume but remains at approximately the same pressure as the surrounding water. Pressure available to the turbines for an underwater bladder system remains constant and is based on the depth the bladders are stored [20], [21]. The use of tanks or bladders removes the geologic limitation found in large-scale systems, allowing for a much broader feasibility for small-scale systems application.

3. Flywheel Energy Storage

Flywheel energy storage (FES) is a means of mechanical energy storage that is best suited for high power output over a short duration [15–17]. Key characteristics of flywheels are “excellent cycle stability and a long life, little maintenance, high power density and use of environmentally inert material” [16]. A typical FES system is shown in Figure 6. It consists of a large cylindrical mass suspended with magnetic bearings in a vacuum chamber [22], [23]. The mass is on a shaft, and one end of the shaft connects to a motor. Charging applies power to the motor, which spins the flywheel up to its design speed. The spinning mass stores kinetic energy as angular momentum [17], [22], [23].

The reason for use of magnetic bearings and a vacuum chamber is to remove as much friction as possible. Any friction present in the system will leach power away from the flywheel, thus reducing its rotation speed. Despite efforts to remove fictional losses, flywheel systems still have a long-term storage problem. Typical flywheel systems experience complete self-discharge in less than a day when they are not recharged regularly throughout the day [15–17]. This indicates that flywheels are not an ideal energy storage method because energy cannot be stored for long durations. However, FES are able to output high power very rapidly making them more suited for use as a power management device [15–17].

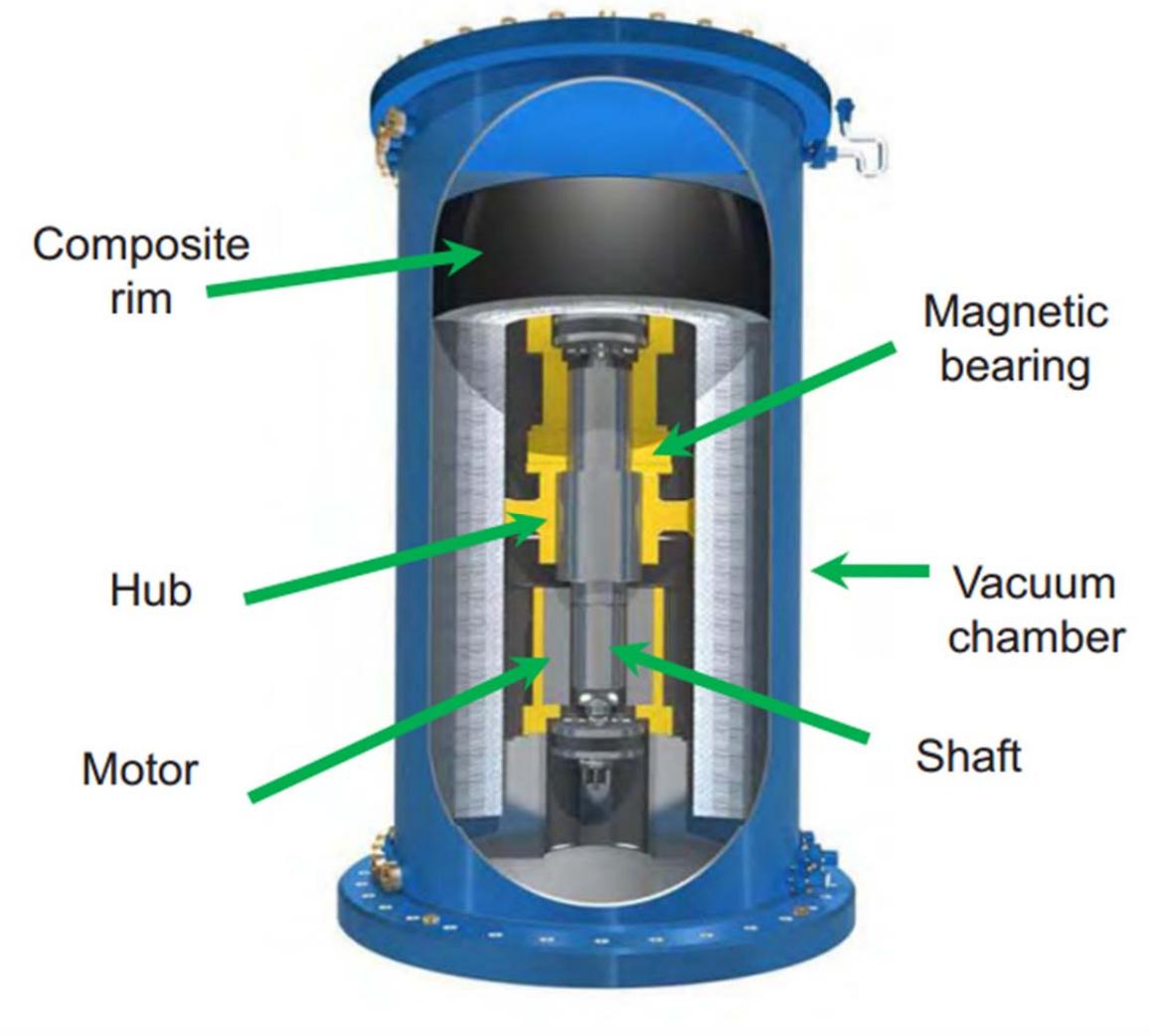

Figure 6 Flywheel Energy Storage Device. Source: [24].

4. Battery Energy Storage System

The electrochemical form of energy storage “is the oldest form of electricity storage” [15]. Electrical energy is stored directly in batteries by reversing an electro chemical reaction. Advantages of batteries include a reasonably rapid response to load variation and very little energy loss while dormant, leading to efficiency from 60 to 95 percent [15], [25]. Batteries have several disadvantages such as limited cycle life, low energy densities, low capacity, and use of toxic materials [15], [25].

There are two types of batteries, secondary and flow, both make use of the same electrochemical principle but have different configurations [15–18]. Many variations of both types of batteries exist with different materials used for the electrodes and electrolyte [15–18].

Secondary batteries are cells consisting of a positive electrode and negative electrode in an electrolyte [15]. The size and composition of the cell determines the storage capacity and the power of the battery following construction. In order to scale secondary batteries to meet the required capacitance and power output individual cells are wired together forming a battery bank [17]. Such a battery bank at the Alaska Center for Energy and Power is shown Figure 7.

Figure 7 Secondary Battery Bank at Alaska Center for Energy and Power. Source: [26].

Flow batteries on the other hand have scalable battery capacity and power output [15-18]. This variability of flow batteries is possible because the cells size can vary,

unlike a secondary battery. A typical flow battery consists of two tanks that store electrolytes, and attached pumps cycle the stored electrolytes through a chamber called a stack. A generic flow battery is shown in Figure 8. In a flow battery the stack is the reaction camber, the stack has cells of positive and negative electrodes [15-18]. The electrolyte in a flow battery is stored in external tanks and pumped into the stack to allow the electrochemical reaction to take place. Flow batteries can scale the capacitance by changing the size of the electrolyte tank storage, and scale the power output by changing the number of cells in the stack [17].

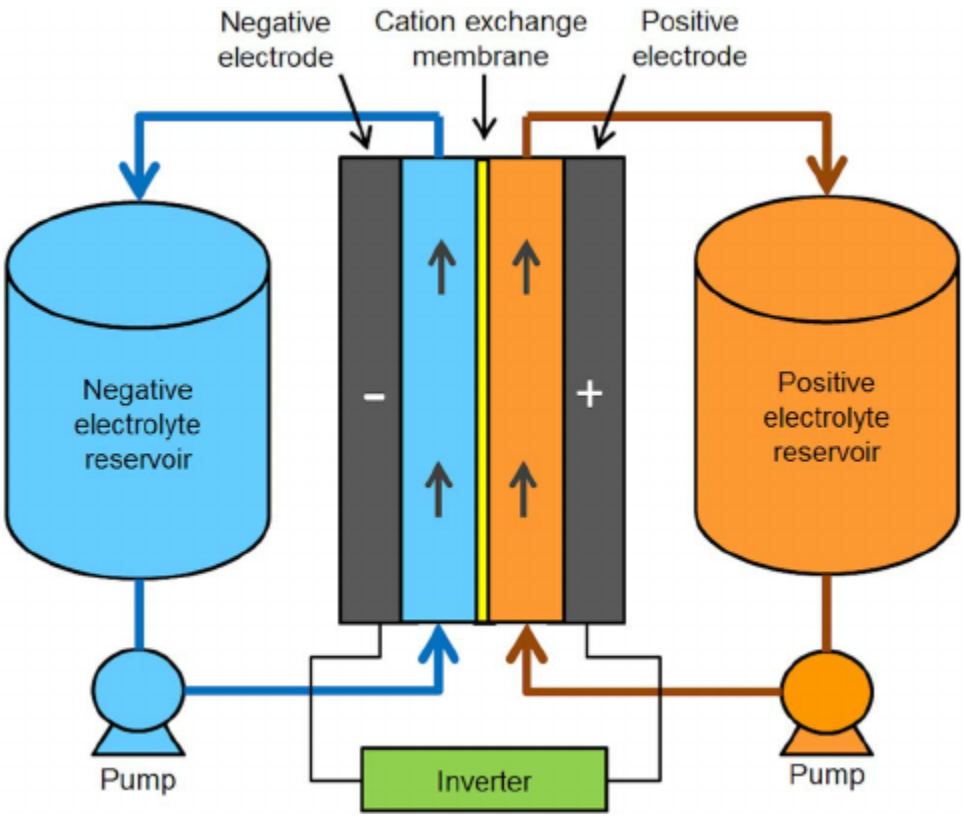

Figure 8 Generic Flow Battery. Source: [27].

Significant research efforts engaged in battery technology with an effort to make them a more viable EES method [15], [25], [28–31]. The focus of much of the research is making a material change to any of the three components: the negative electrode, positive electrode, or electrolyte. Much of this research endeavors to improve capacity or power

output, less attention has been given to making batteries with fewer toxic materials [28]. The majority of commercially available batteries are not suitable for long-term use in EES, due to material used in their construction and their lack of recyclability [28].

5. Hydrogen Storage

Excess electrical energy in the form of chemical energy, in the form of hydrogen and synthetic natural gas (SNG), is cable of storing vast amounts of energy for lengthy periods. Hydrogen and SNG is an attractive EES because it "is the only concept which allows storage of large amounts of energy, up to the TWh range, and for greater periods of time—even as seasonal storage" [16]. One favorable aspect of hydrogen and SNG is its versatility for use as transportation and heating fuel [16], [32]. In addition, it is possible to modify certain fossil-fueled electric generators currently using natural gas to make use of the renewable hydrogen or SNG [33].

The process of storing excess in the form of chemical energy is less direct than most other methods. To create hydrogen excess electrical power energizes an electrolyzer that splits water into its constituents, hydrogen and oxygen. Typically, hydrogen is then stored in tanks or caverns and the oxygen is exhausted to atmosphere. The oxygen is not generally stored for practical and economic reasons. If the oxygen were stored, additional tanks or caverns would be required [16]. SNG, synthetically produced methane, production involves combining the hydrogen produced through electrolysis with carbon dioxide in a methanation reactor [16]. The SNG is then stored in the same manner as hydrogen systems.

Storage of the working fluid is the limiting factor for implementation of hydrogen and SNG. Like CAES, hydrogen and SNG EES require very large storage tanks or caverns to be viable [32]. In order to have large-scale hydrogen or SNG storage the use of appropriate underground geological formations such as "depleted gas/oil reservoirs, aquifers, and salt caverns" is required [34]. Due to the similar storage requirements of CAES, hydrogen and SNG compete for space. When it comes to power generation in the few gigawatt range, CAES is currently viewed as a more suitable use of the storage sites because it has a higher efficiency, and lower capital investment and operating costs [32].

Some possible underground storage methods for hydrogen, SNG, and CAES are shown in Figure 9.

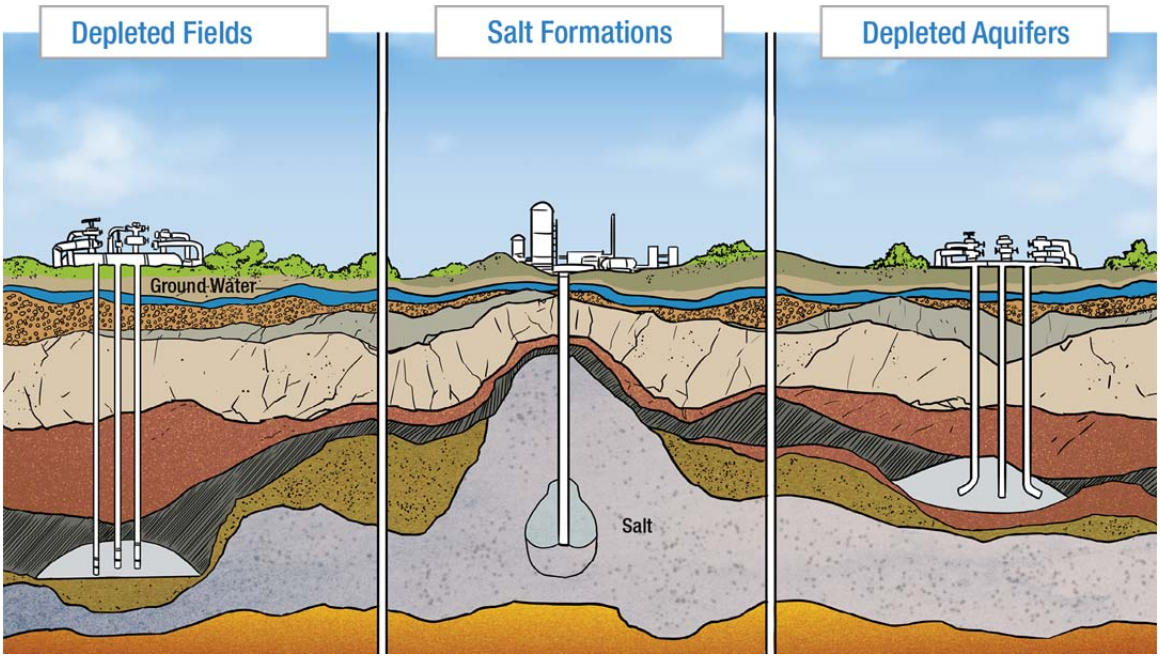

Figure 9 Some Suitable Underground Storage Methods for Hydrogen, SNG, and CAES. Source: [35].

Chemical energy storage technologies are better suited for a more compressive storage method, such as storage for an entire nation or world power grid. A study completed by SIEMENS & ISET investigated the required storage capacity that would be necessary for Europe's entire power grid to subsist on solar and wind resources [32]. Hydrogen storage would require 167 TWh, over twice the energy storage necessary for PHS or adiabatic CAES [32], [36]. However, 0.41 km^3 is the volume required to achieve the prescribe capacity, which is seventy times less than what is necessary for the nearest storage competitor Adiabatic CAES at 29 km^3 [32,36]. This indicates that hydrogen storage is best suited for a national grid scale application despite having a lower efficiency than PHS and CAES.

6. Electric Double Layer Capacitors and Superconducting Magnetic Energy Storage

The use of electric double layer capacitors (EDLC) is the most direct means of electrical storage. EDLC are a highly efficient, rapidly chargeable EES method [15–17]. Storage using EDLC is scalable which enable systems capable of producing up to 300 kW [15]. In response to a changing load EDLC are capable of responding very rapidly [15–17]. Self-discharge rates of EDLC of around 40% per day make them most suitable of storage of energy from seconds to hours [15].

EDLC have quite a simple design, consisting of two plates with a small space occupied by a material known as dielectric. One of the plates is positive and one is negative. Charging an EDLC causes electrons to migrate from the positive plate to the negative plate [17]. When the charging sources are removed, the negatively charged plate has more electrons than the positively charged plate, creating an electrical potential. Upon loading, the EDLC electrons attempt to achieve balance in both plates, and thus flow from the negatively charged plate back to the positive, resulting in an electrical discharge [17]. A visual representation of the charging and discharging process of an EDLC is shown in Figure 10.

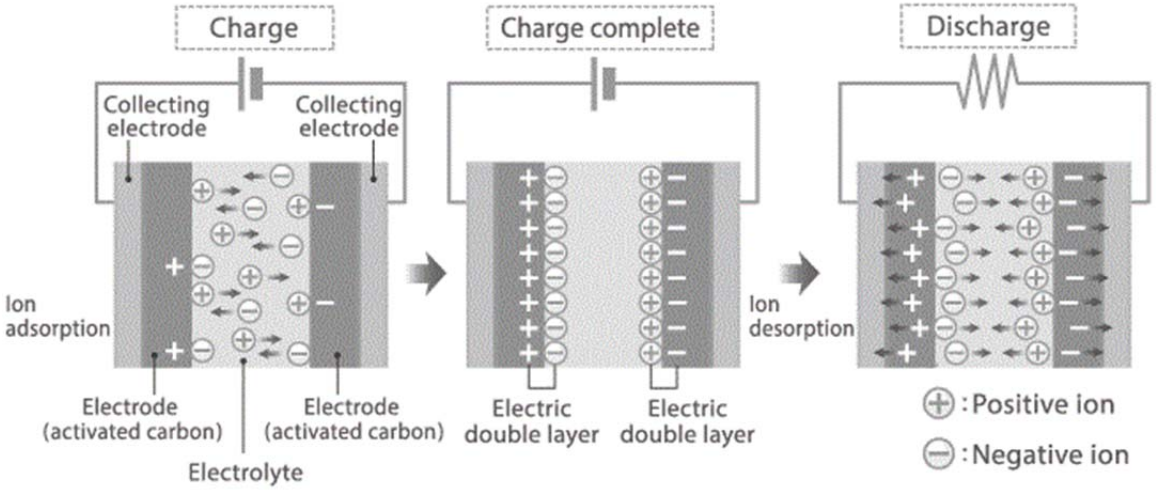

Figure 10 Charge and Discharge Process for EDLC.
Adapted from [37].

Superconducting magnetic energy storage (SMES) is an emerging method of storing electrical energy in the form of electrical current [15–17]. SMES has many of the same advantages as EDLC. SMES has a slightly higher roundtrip efficiency of about 95%, compared to 90 % of DLC [15–17]. The expected lifetime of SMES is at least 20 years, twice that of EDLC, due to SMES not having cycle limits [15–17]. The power rating of SMES is up to 10 MW, significantly higher than that of EDLC [15]. The response time of SMES to a load is nearly instantaneous [15–17]. Although slightly less than EDLC, self-discharge in SMES systems is an issue at around 15% per day [15].

SMES is a much more complex storage system than EDLC. Typically, a SMES consists of a coil of super conducting material suspended in a cryogenic chamber filled with super cooled helium. A conceptual design of a SMES is shown in Figure 11. Several auxiliary systems are required to maintain the helium at cryogenic temperatures around 4.5 K [15]. Charging a SMES creates a magnetic field in the cryostat chamber by passing current through the coil [15–17]. The energy is stored in the magnetic field and current continues to flow through the coil after the power source has been removed [15–17]. The magnetic field induces a current through the coil. A load draw on this current depletes the magnetic field.

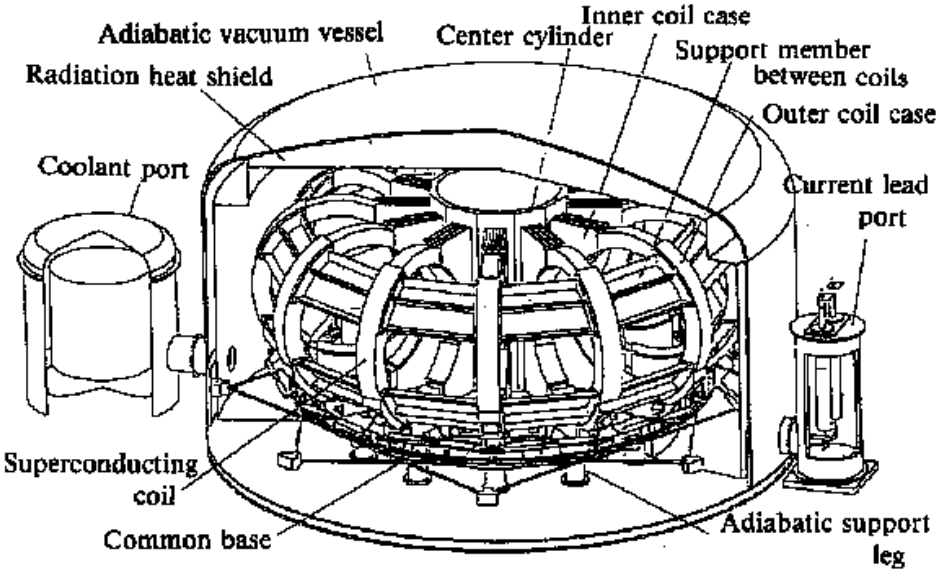

Figure 11 Conceptual Design of a Small-Scaled SMES. Source: [38].

Due to the rate of self-discharge of EDLC and SMES, neither is well suited as a bulk long-term EES method. EDLC and SMES are more suited to power management enabled by rapid discharge rates. Typically, the materials used to construct EDLC and SMES are benign and easily recyclable [15–17]. However, there is concern regarding the environmental impact of the large magnetic fields produced by SMES [15–17]. SMES is much more expensive to produce and maintain than EDLC [15–17]. Based on the significant price difference and environmental concerns for SMES, EDLC may be the preferred option of the two systems for power management of sustainable power systems.

7. Thermal Energy Storage

Thermal energy storage (TES) systems store heat in three forms: sensible, latent, and thermo-chemical [16]. Most industrial or residential TES is in the form of sensible or latent [16], [39]. Heat is stored in the form of low-temperature to be used for cooling later or high-temperature to be used for heating [15]. All cases make use of thermally insulated containers [15]. The round trip efficiency of TES systems is quite low, ranging from 30 to 60 % [15]. However, in several cases the energy stored using TES would otherwise be wasted. For example, heat generated during compression of air in a non-adiabatic CAES can be stored to create a near adiabatic CAES. TES systems are environmentally benign and can store otherwise wasted energy, making them a valuable addition to a renewable EES.

Sensible heat storage makes use of an inexpensive storage medium with high specific heat capacity [39]. When heat is stored as sensible heat an appreciable change in temperature of the medium is observable. Some typical storage media are water, rock and metals [16], [39]. Recovery of the stored heat from solid storage requires passing working fluid through the storage medium in the containment camber [15], [39]. When heat is stored in fluid heat recovery may involve pumping the storage medium out of the containment vessel to an external heat exchanger [15], [39]. Alternatively, a heat exchanger may be located inside the fluid containment vessel and have a working fluid pumped through to recover heat [15], [39].

Latent heat storage takes advantage of the phase change of the storage medium to store heat. Since energy is stored with a phase transformation, there is not a significant change in temperature of the medium [16]. The mediums used for latent heat storage are more numerus than those of sensible heat storage. Selection of the latent TES medium is based on its melting or boiling point [39], [40]. Whether the melting or boiling point is the criteria for selection depends on the required phase transformation: solid-to-liquid, liquid-to-gas, or liquid-to-solid [39], [40]. Options for latent mediums include both organic and inorganic materials. Some commonly used mediums are water, paraffins, salt hydrates, and non-paraffin organics [39,40]. Recovering the heat from the latent storage medium typically requires a working fluid pumped through a heat exchanger within the containment vessel [15], [16], [39], [40].

Standalone use of TES as an EES is best suited to solar concentrators where excess heat produced during the day is stored to allow continuous power generation through the night. A solar concentrator with attached TES tanks is shown in Figure 12 [16], [41]. Use of TES in conjunction with other EES methods provides clear benefits, such as storing heat that would otherwise be wasted and increasing efficiencies. In the case of an adiabatic CAES using TES to store heat produced during compression, that would otherwise be lost, enables the creation of high power sustainable EES [16].

Figure 12 Solar Concentrator Tower and TES Tanks. Source: [42].

D. MEETING NAVY ENERGY GOALS

Utilization of EES is the key to meeting the SECNAV's priority of energy independence. To achieve 100% energy independence, microgrids generating power using solar, wind, and marine resource need to integrate sufficient EES to meet demand at all times. Similar to traditional energy production methods, there is no singular EES solution, and most applications would benefit from a combination of EES methods. One such EES combination would be the incorporation of adiabatic CAES, TES and EDLC into DON installation microgrids, which would lead to energy independence with the added benefit of being environmentally benign.

Many DON installations are located near the sea, so the geologic requirements for standard underground CAES can be subverted through the use of undersea CAES. The power demand on DON installations ranges from tens to hundreds of MW [3], [43]. The bulk storage of energy with CAES would be capable of meeting the demands of the installations with a power rating of 5–300 MW [15]. CAES has the advantage of being one of the cheapest high-power output bulk energy storage methods at 2–50 $/kWh [15].

To create an adiabatic CAES, heat generated during compression of air would be stored with TES. Use of an EDLC for power quality and management would allow for response to sudden loads on the microgrids.

While the DON is still investigating large-scale grid EES options, presently small-scale CAES exist on many DON installations and assets. On many bases and all naval vessels, compressed air is stored for industrial use. Using these preexisting compressed air storage systems for small-scale CAES would enable peak shaving and emergency power during outages. Peak shaving could reduce the required maximum power generation of the microgrid. In addition, peak shaving would reduce costs for DON installations on the standard gird. Power use during a peak demand period lasting from 15 minutes to one hour could account for up to 50% of a facility's power bill [44]. Additionally, the use of small-scale CAES (SS-CAES) generation for emergency power during outages could provide energy security to installations.

E. SS-CAES AT NAVAL POSTGRADUATE SCHOOL

At the Naval Postgraduate School (NPS) Integrated Multi-Physics Energy Lab (IMPEL), a proof of concept SS-CAES has been undertaken. NPS IMPEL is a DON installation with a preexisting compressed air storage system. The intention of the proof of concept is to develop a SS-CAES system that is scalable, enabling application at other DON facilities.

Previous work on the SS-CAES project has led to the installation of a scroll compressor powered by a solar microgrid [45]. Originally, the compressor required manual operation and only featured analog control via a dropout relay. Later work has enabled autonomous operation of the compressor [46]. The scroll compressor operates autonomously when sufficient electrical power from the installed solar panels is available. The installed solar panels at NPS IMPEL are shown in Figure 13.

Figure 13 Solar Panel Array and Vertical Axis Wind Turbine at NPS IMPEL

The air generated by the solar-powered compressor is stored in four large preexisting compressed air tanks. A supersonic wind tunnel at NPS IMPEL uses the air stored in these large tanks to operate. The supersonic wind tunnel experiences only occasional use. Thus, utilization of the tanks for CAES during periods between the wind tunnel's operations would optimize the tanks' potential. The four compressed air storage tanks installed at NPS IMPEL are shown in Figure 14.

Figure 14 Four Large Compressed Air Storage Tanks at NPS IMPEL

Work on electrical generation using stored compressed air has been done, along with the previous work on the compression side of the SS-CAES system. The electrical generation method developed uses a turbine attached to a generator to produce electricity, shown in Figure 15 [47]. Stored compressed air is used to power the turbine, which in turn spins the generator, producing three-phase AC with wild frequency. The three-phase AC voltage passes through a bridge rectifier creating DC voltage, used to charge super capacitors. Like the scroll compressor, the turbine and generator require manual operation.

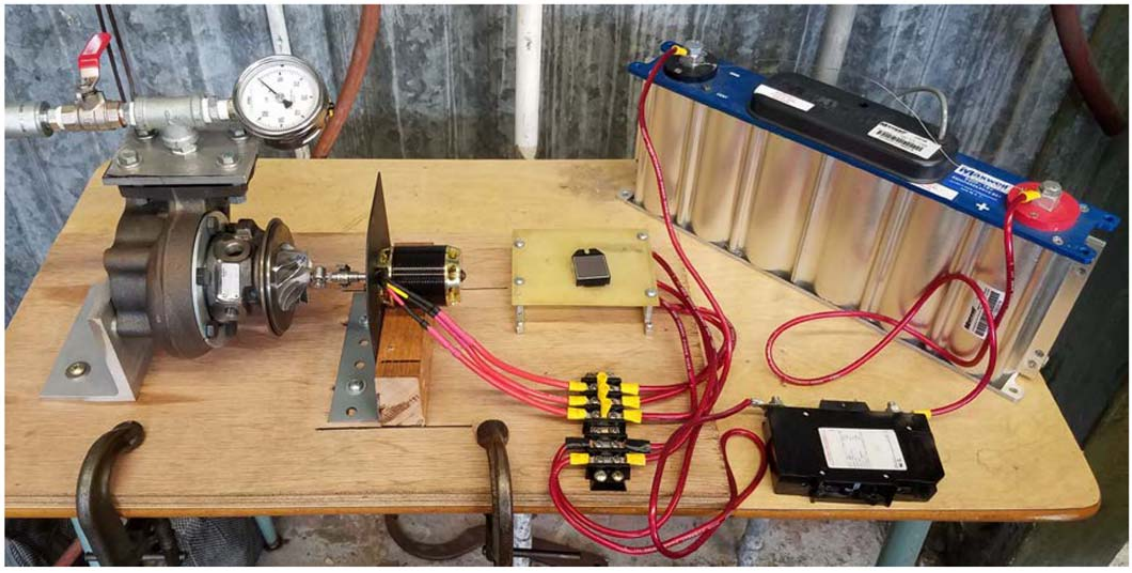

Figure 15 NPS IMPEL SS-CAES Generator Developed Previously. Source: [47].

F. MOTIVATION

The aim of this thesis is to progress the work on the SS-CAES at NPS IMPEL. The primary objective is the development of a control system for the electrical generation side of the SS-CAES. The purpose of the control system is to enable autonomous operation of the electrical generator in response to a load. A secondary objective of the design is a robust control system enabling integration into the NPS IMPEL proof of concept SS-CAES system as well as other SS-CAES applications. An additional secondary objective of the design is to create a control system capable of a dark start to enable operation of the control system in the absence of an external power source. With endeavors to reduce future production costs, the design intends to develop a control system that can be programmed and then stored for long periods, allowing for batch production.

II. COMPONENT SELECTION

A. CONTROLLER

The choice of controller requires understanding of its prospective application. In this case, the expectation is that sailors and marines would use the SS-CAES in industrial environments. Given the intended operators, a controller that is intuitive and user friendly is required. In addition, since the operators are not necessarily technical experts regarding controllers, the controller should not require significant maintenance or modification by the users. The working environment for the controller might be subject to temperature extremes, dust, salt, and moisture. The controller may be integrated within an inhospitable environment. This requires the control hardware to be robust. Additionally, a controller that consumes low power is preferable. An industrial programmable logic controller (PLC) fulfills the requirements for application in a SS-CAES system.

PLCs are available in many sizes and input/output configurations. Narrowing the choice of which PLC is best suited for this application involves considering the type and number of inputs and outputs. In most cases, inputs and outputs are analog or digital. As well as the input/outputs, consideration of the human machine interface (HMI) is also a decision factor. Preliminary examination of the control system revealed that two to five analog outputs and one to three digital inputs would be required for the SS-CAES proof of concept at IMPEL. Since the operators are not expected to be technical experts, an HMI with a visual display that is intuitive and easily comprehended is required. Many PLCs have no built-in HMI; they have no visual display and require the installation of buttons. Several PLCs do have visual displays using lights and single-line text screens, but they still require the installation of buttons. Some PLCs have touch-sensitive screens that can both display various conditions and act as buttons, making them ideal for this application.

For use on the power generation side of the SS-CAES system at NPS IMPEL, selection of a PLC with at least five analog outputs, two digital inputs, and a HMI with a touch sensitive screen is required. A controller is also required for the compressor side of

the SS-CAES system at NPS IMPEL. For convenience, both sides of the SS-CAES system at NPS IMPEL would use the same controller [46]. Combining the requirements of the two sides of the SS-CAES system at NPS IMPEL led to the selection of the PLC. Both sides of the SS-CAES system at NPS IMPEL will use the Allen-Bradley Micro850 PLC, shown in Figure 16. This controller is robust enough for industrial applications, consumes approximately 10 watts (W), and has many additional inputs and outputs for later expansion of the project.

Figure 16 Allen-Bradley Micro850. Source: [48].

1. Micro850 Inputs and Outputs

The Micro850 has input and output buses, top and bottom, respectively; green terminal strips shown in Figure 16. All inputs and outputs through the sustainable bars are digital. There are fourteen 24 volts (V) direct current (DC) or alternating current (AC) inputs and ten 24V DC source outputs [48]. The Micro850 controller requires plug-in modules for input and output analog signals. The module plugs into one of the three covered expansion blocks shown in Figure 16. A typical expansion block is shown in Figure 17. The expansion block used for SS-CAES is the 2080-IF2, which is a non-isolated unipolar voltage/current analog input [49]. The 2080-IF2 measures analog voltage input in this case; it has two inputs capable of sensing zero to ten volts.

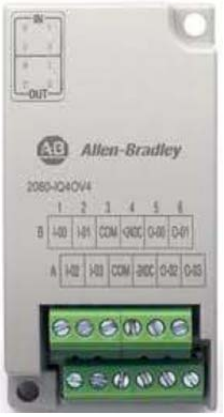

Figure 17 Micro800 Series Expansion Block. Source: [48].

2. Micro850 Human Machine Interface

The Micro850 is capable of operation using just the controller shown in Figure 16 but with the addition of a 4-inch touch-sensitive screen, PanelView 800, it is much more user friendly. On the left side of the Micro850 there are indicator lights. Upon sensing an input, the input lights illuminate and the output lights only illuminate when an output signal is energized. There are also several status lights. The use of a display screen allows the system developer to create displays that enable users to understand the status of the system without being technical experts. Increased functionality in the form of buttons on the display enables the system developer to allow the user to interact with the system in a predefined manner. With the use of the PanelView 800, shown in Figure 18, the user only needs to interface with the screen in order to operate the controller and attached system. Since the user only needs to interface with the HMI, it is possible to obscure all wiring and control components in an enclosure.

Figure 18 PanelView 800. Source: [48].

B. VOLTAGES

There are two working voltages in the control system. The first is the voltage source for the system components. The second is the control voltage, which provides a signal to control components.

1. Power Source Voltage

There are three power source options for most controllers and control components, 24V DC, 120V AC, and 240V AC. 24V DC is favorable, but due to the nascent developmental stage of the SS-CAES system at NPS IMPEL, that voltage source would not be available. Instead, 120V AC is used for the controller and control components. This voltage allows the use of standard power from outlets, which is convenient for the development of the SS-CAES system.

2. Control Voltage

The Micro850 has an attached power supply that converts a 120V AC source voltage to 24V DC, and uses the 24V DC from the power supply to operate. The output, or control signals, from the Micro850 are also 24V DC. Therefore, actuation of all control components is via 24V DC. The control signal from the Micro850 is approximately one amp [48]. Due to the low amperage of the control signal, the Micro850 is not capable of powering most control components directly.

C. CONTROL COMPONENTS

Control systems require various components to sense and physically manipulate a working fluid or machinery. For this system, compressed air is the primary medium controlled, which requires the use of solenoid valves and relays. The primary input to the control system is the voltage of a capacitor, which necessitates the use of voltage transducers. The componentry combines to form a functional control system.

1. Solenoid Valves

Solenoid valves have a coil that creates a magnetic field when energized that moves an actuator or armature to change the state of the valve. Two methods of operation exist for solenoid valves, direct acting and internally piloted. Direct acting solenoid valves receive sufficient power from the coil directly to move and maintain the position of the valve. Internally piloted solenoid valves do not use the coil's power directly to change the valve position. Instead, the coil changes the position of a smaller pilot valve allowing working fluid to move through the valve body to change the main valve's positon.

A direct relationship between power consumption of direct acting solenoids and the pressure differential the valve must overcome exists. This relationship limits the direct acting valve's application to smaller lower pressure systems. Internally piloted valves, on the other hand, have no such relationship; their power consumption falls within a fixed range. The use of a pilot valve enables internally piloted valves to work in high-pressure applications. Also, internally piloted valves consume less power than direct

acting valves for the same application [50]. This limitation to internally piloted valves does not exist in direct acting valves. Internally piloted valves require a pressure differential across the valve to operate. For example, energizing a completely disconnected valve will not shift its position. A direct acting valve, on the other hand, will shift regardless of pressure on either side of the valve.

There is further classification of solenoid valves by the number of ports they have as well as their un-energized position. “#-way” describes the number of ports a valve where “#” is the number of ports. Description of the de-energized state of the valve is either normally closed (NC) or normally open (NO). For example, a typical direct-acting solenoid is two-way NC, meaning one input and one output, which opens when energized. Additionally, a typical internally piloted solenoid is three-way NO, meaning one input and one output, and one exhaust, which closes when energized.

The operating pressures for the SS-CAES at NPS IMPEL would not be too great to use direct acting solenoids. Internally piloted solenoids were selected for use in the SS-CAES because they use significantly less power than the direct acting solenoid alternative. The control system makes use of both three-way NO and NC internally piloted solenoids with source voltage selected, 120V AC. The solenoid valves used are Parker B6 series shown in Figure 19.

Figure 19 Parker B6 Piloted Solenoid Valve. Source: [51].

2. Relays

Since control components, such as solenoid valves, require more power than provided by the control signal from the PLC, relays must be used. Relays enable the control of high voltage and high amperage circuits while using very small electrical signals to turn them on or off. A relay is an electronic switch that opens or closes an electrical contact when energized. In this case, the control signal from the PLC energizes the relays causing them to change the state of the electrical contact from open to closed, or vice versa. The contact controlled by the relays is in the power circuit for control components, which is receiving power form the 120V AC power source. For example, a solenoid valve that is powered by 120V AC has a normally open relay in-between the power source and the solenoid. When the relay receives a control signal the circuit closes and the valve changes position.

Several types of relays are available, the most commonly used are electromagnetic and solid-state relays (SSR) [52]. Like solenoid valves, electromagnetic relays make use of a coil to induce a magnetic field to move an armature that changes the position of the contacts in the relay. An electromagnetic relay, which has one normally open and one normally closed contact is actuated by the white armature attached to the coil shown in Figure 20. Solid-state relays do not have any moving parts. Instead, internal circuitry changes the state of the contact when a control signal is present. Although they are able to control high-power devices, these relays consume very little power themselves. Both types of relays require approximately 1W of power, with SSR generally consuming slightly less than electromagnetic relays [53], [54]. Besides the reduced power consumption, a main advantage of SSR over electromagnetic relays is there are no moving parts, making SSR more robust with longer life spans. Most SSR have a single contact that is normally open. Electromagnetic relays are widely available with multiple contacts, some normally closed and some normally open, on the same relay.

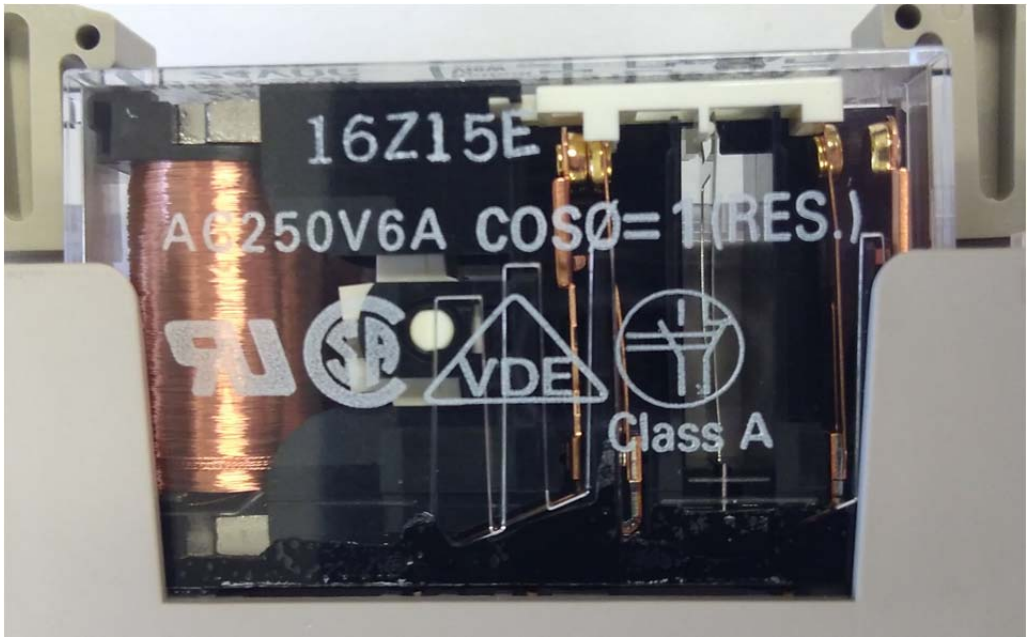

Figure 20 Electromagnetic Relay

The control system mainly makes use of relays to control power to solenoid valves. The valves operate independently of each other, meaning only relays with one contact are required. In addition, the valve selection enables the use of normally open relays. The use of SSR is favored for the control system because of their simplicity, robustness, and longevity. In all instances where a relay is needed in the control system, a single contact relay is sufficient. When normally open relays are required, SSR are preferred. Only when normally closed or multiple contacts are required should an electromagnetic relay be utilized. The SSR primarily utilized are Crydom D2450; the control input range is 3–23V DC and output up to 50 amps at 240V AC.

3. Voltage Transducers

The main input signal to the controller is voltage measurements. Of the two types of input signals to the controller, analog or digital, variable magnitude is sensed only on analog inputs. Thus, the voltage reading inputs must be input via the analog module on the PLC. The analog module has a limited input sensing range of 0–10V DC. However, input voltages sensed are higher than ten volts. To facilitate measuring voltages higher than ten volts, utilization of a voltage transducer is required. A voltage transducer

converts the higher voltage input into to a lower voltage signal. The input and output of the transducer are isolated from each other so there is no risk of applying too much voltage to the analog module. Selection of a voltage transducer with a wide input range allows future flexibility. Both the air compression and the electrical generation constituents of the SS-CAES at NPS IMPEL utilize CR Magnetics CR5311-75 voltage transducers, shown in Figure 21. The CR5311-75 has an input range of 0–75V DC, an output range of 0–10V DC, and requires supply power of 24V DC.

Figure 21 CR Magnetics CR5311-75 DC Voltage Transducer

Accuracy of the voltage transducer is important in order to prevent placing the capacitor in an overvoltage condition, which would significantly reduce the life span of the capacitor in the SS-CAES system. According to the manufacturer, the CR5311 has a response time of 250 microseconds and an accuracy of 1.0% [55]. The maximum voltage of the capacitor in the SS-CAES generator previously developed is 17 V or 6.25% of the working voltage [47], [56]. Thus, accuracy of the voltage transducer is sufficient to prevent the capacitor from being placed in an overvoltage condition.

D. MANUAL COMPONENTS

To enable manual operation of the generator, a manual valve is required to bypass the autonomous manifold. The manual value is necessary for operating the system when no electrical power source is available, or for testing. Inadvertently leaving a manual bypass valve open with the system running using the controller would disable autonomous operation by allowing the generator to run continuously. Unintentionally running the generator continuously would eventually lead to overcharging the electrical energy sinks connected to the generator. The electrical energy sinks used for the SS-CAES at NPS IMPEL are ultra-capacitors. While safer than overcharging batteries, overcharging capacitors is still problematic because it reduces their lifespan and effectiveness [57], [58]. To prevent the manual valve from remaining open inadvertently, a valve with spring return handle is required. The valve selected is an Apollo Valves 71–502-01, shown in Figure 22, which is a ball valve with a spring return handle.

Figure 22 Apollo 71–502 Series Valve. Source: [59].

III. SYSTEM ARCHITECTURE

A. SYSTEM LAYOUT

A schematic of the control system designed to enable autonomous operation of the SS-CAES generator is shown in Figure 23. A dashed box encloses the components of the generator that had been previously designed in a past iteration of the SS-CAES project at NPS IMPEL [47].

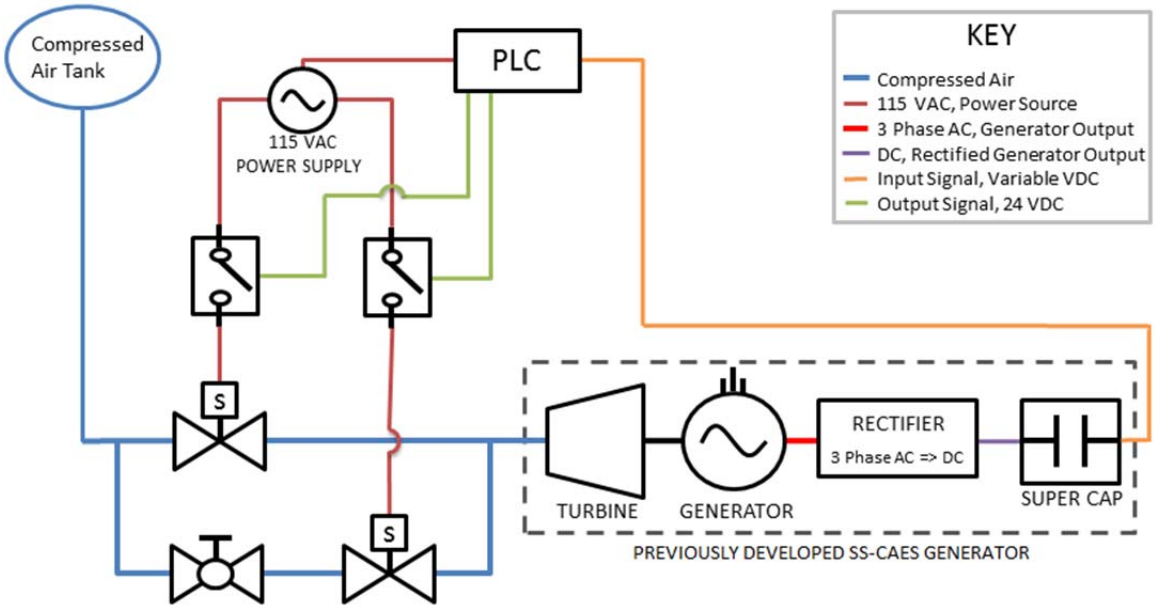

The dashed box encloses the components of the generator that had been previously designed in a past iteration of the SS-CAES project at NPS IMPEL [47].

Figure 23 SS-CAES Generator Schematic

1. Power Supply

The power supply consists of a power strip plugged into a wall outlet supplying 115V AC. Plugged into the power strip are control components that require external power: the Micro850 controller and two solenoid valves. The connections to the power supply by these components are shown by dark red lines in Figure 23. The relays make breaks in the dark red lines leading to the solenoid valves, since the relays act as switches between the power supply and the solenoids.

2. Compressed Air System

All the fittings for the valves and piping used in the air system have 3/8-inch national pipe thread (NPT). For convenience during the development of the SS-CAES, industrial/Milton quick connects are used to connect the air control manifold to the compressed air supply and the turbine. Half-inch air hose attached to barbed hose fittings connects components in the compressed air system. The blue lines in Figure 23 illustrate the compressed air piping and connections. The compressed air system for the SS-CAES at NPS IMPEL is shown in Figure 24.

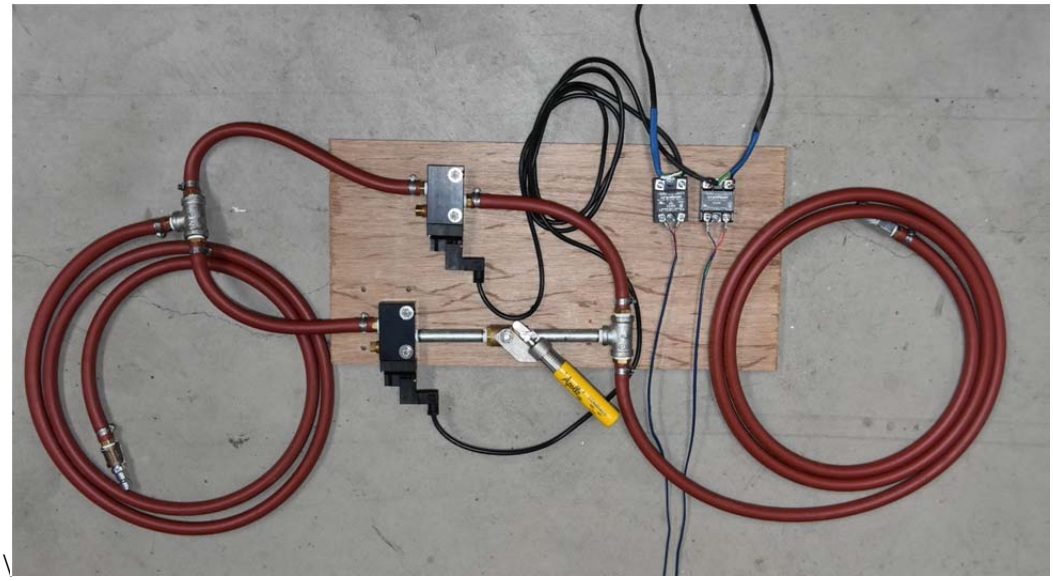

Figure 24 Compressed Air System for SS-CAES

The control manifold has two parts, one automatic and one manual. The control manifold is shown in the bottom left of Figure 23. The two valves on the lowest blue line represent the manual segment, and the piping and valve above is the automatic segment. The manual portion of the air manifold consists of a manual valve followed by a solenoid valve configured to be normally open. The assembled control manifold is shown in Figure 25. Configuration of the manual side solenoid valve as normally open enables the use of the generator without any external power or control outputs from the Micro850. Manual operation of the generator only requires opening the spring return valve.

Releasing the spring return handle will immediately cease the generator's operation. The automatic part of the manifold has a normally closed solenoid valve configuration. For autonomous operation, the Micro850 sends a control output to the relay attached to the automatic solenoid, which closes the circuit between the power supply and the solenoid, and opens the valve.

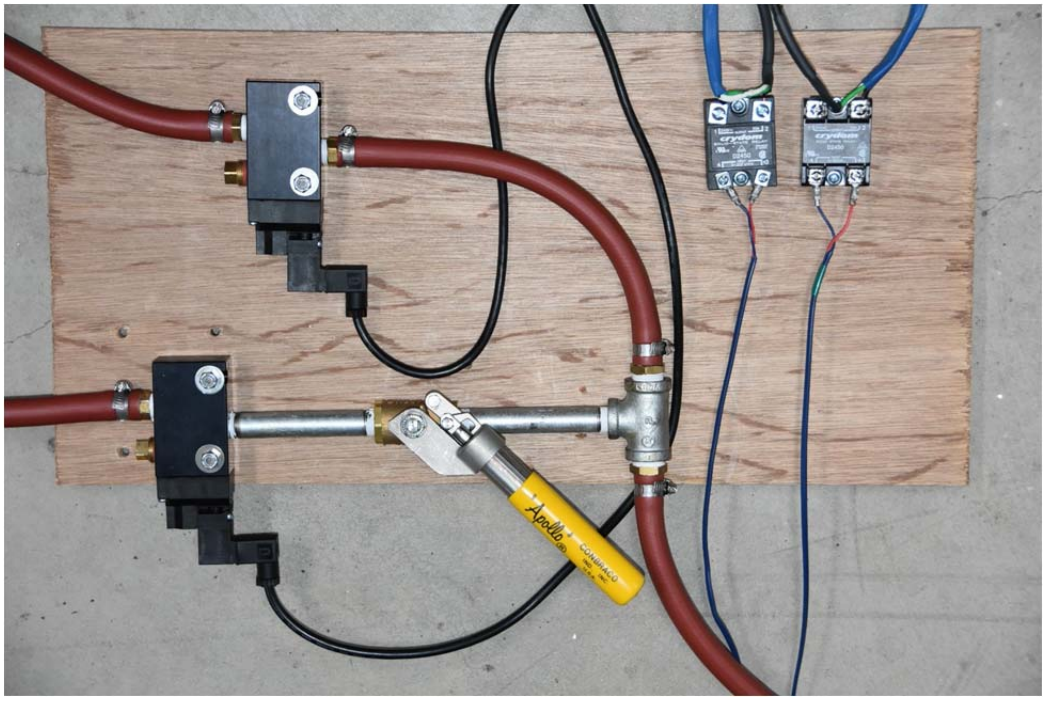

Figure 25 Control Manifold

3. Signals

The 24V DC control output signal from the Micro850 is shown as a green line in Figure 23. The control output is simply connected to the relays using wire.

The input signal to the Micro850 is the variable DC voltage of the capacitor shown by the orange line in Figure 23. The voltage of the capacitor ranges from 0–16V DC, exceeding the maximum input voltage of the Micro850, and cannot be sensed directly. Instead, a voltage transducer reconciles the signal. The inputs of the voltage transducer connect directly to the capacitor, and the output of the voltage transducer connects to the analog input of the Micro850. Finally, the signal received by the

Micro850 undergoes analogue to digital processing using a function block that converts the signal into an integer representing the voltage of the capacitor.

B. CONTROL PROGRAM

A proprietary software called Connected Component Workbench (CCW) is required to program the Micro850. Three methods of programming in CCW are available: ladder diagram, function block, and structured text editors. Function block was the programming method used for the development of the control algorithms for the SS-CEAS project. Programming using the function block editor is marginally more intuitive than the other two editors, which is what led to its adoption for the SS-CEAS project.

The Micro850 begins running its control programming as soon as it is powered on. This allows the Micro850, if programmed to do so, to control processes immediately after being powered on and without needing an operator to start the controller. Despite this possibility, the control program for the operation of the SS-CEAS generator does require operator input to begin autonomous operation. Immediate autonomous operation is undesirable during development of a control algorithm.

The control algorithm developed for the SS-CEAS has three inputs: two operator inputs, and one measured input. The operator input is in the form of buttons programmed onto the HMI. The buttons are Emergency Stop and Autonomous Run toggles. The measured input is the voltage of the capacitor. The program uses these three inputs combined with program variables to determine what state in which to put the solenoid valves. Two important program variables are the upper and lower bounds of the acceptable voltage range of the capacitor. The SS-CEAS proof of concept at NPS IMPEL has a 16V DC capacitor installed, so the upper bound is 16V DC and the lower bound is 13V DC. A simplified flowchart of the control algorithm developed for the SS-CEAS is shown in Figure 26.

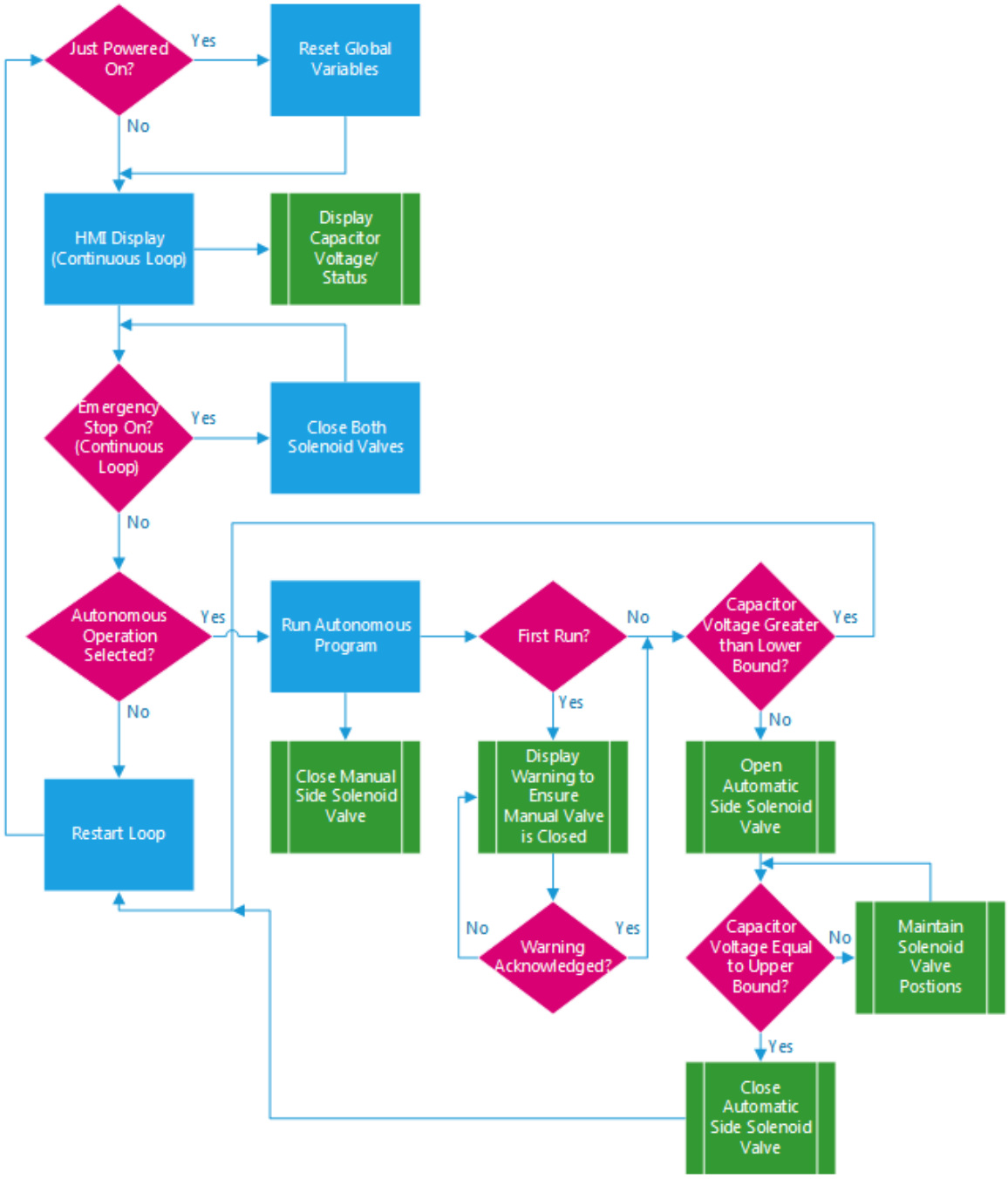

Figure 26 Control Program Flowchart

1. Resetting Variables

The Micro850 has internal memory that stores the last state of variables when power is secured. This can create a problem when power is restored because variables

may have been stored in a state that is not desired at the beginning of operation. Therefore, it is desirable that all the variables used in the control programing of the Micro850 begin in the same state every time it powers on. The use of a variable built into the Micro850 by the manufacturer enables the reset of program variables. When first powered on, this variable indicates true. Then, a short program resets the program variables.

2. Human Machine Interface

As soon as it is powered on, the HMI displays the capacitor voltage level referenced to the upper bound of the capacitor voltage via a graphic bar display. In addition, a status in the form of a colored box with text is also present on the display, as an alternate indication of the capacitor voltage. If the capacitor's voltage is below the lower bound voltage, the indication is "Low" in a red box. If the capacitor's voltage is above the lower bound voltage, the indication is "Good" in a sustainable box. The low and adequate voltage indicators are shown in Figure 27 and Figure 28, respectively.

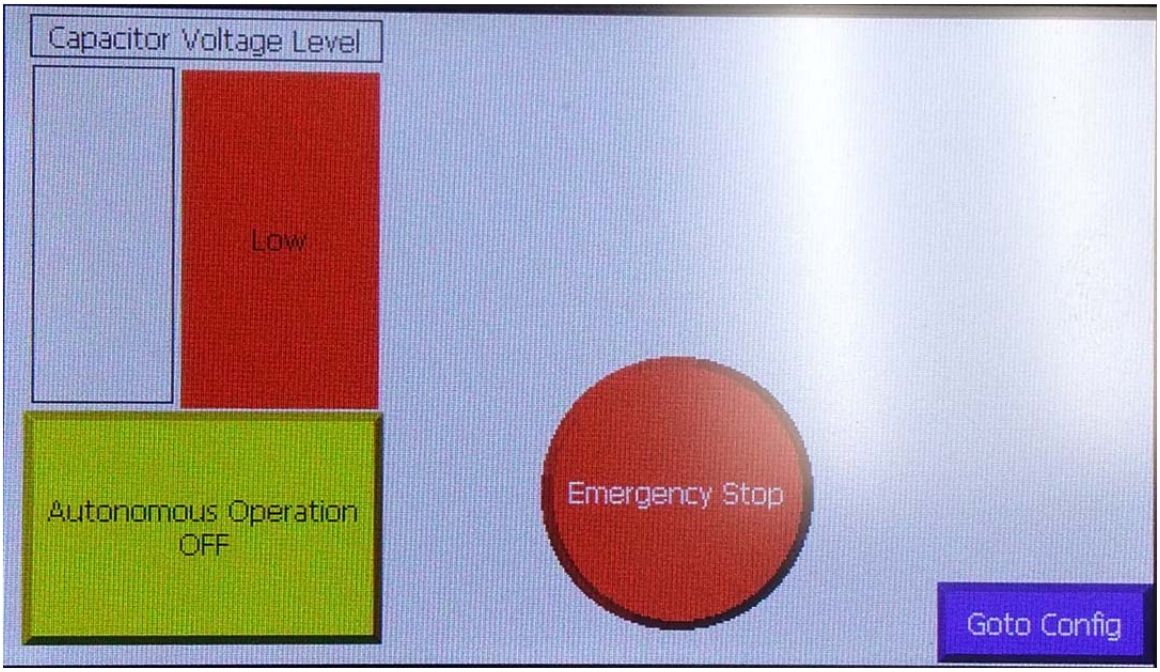

Figure 27 HMI Low Voltage Indication

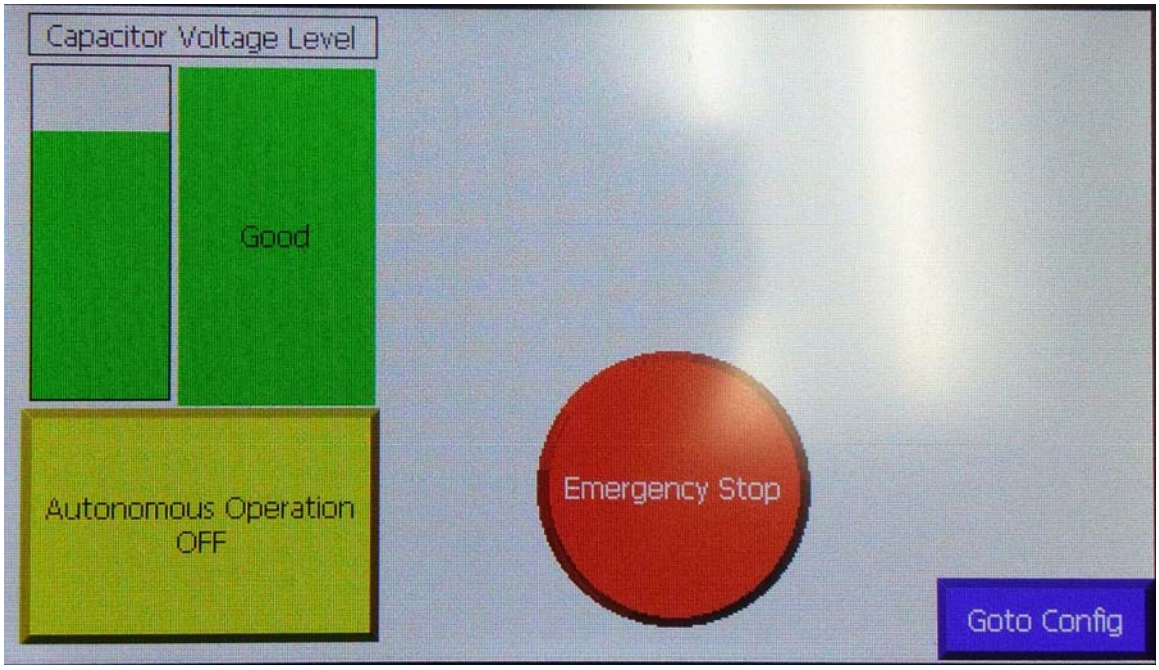

Figure 28 HMI Adequate Voltage Indication

Also, once the HMI is powered on, the user input toggle buttons, Emergency Stop and Autonomous Run, become visible. Engagement of either button changes its text and color. The two configurations of each user input button are shown in Figure 29 and Figure 30. The buttons are linked to Boolean program variables whose state changes from false to true when the buttons are depressed. The flowchart shown in Figure 26 denotes the Boolean variables as diamonds where true and false are represented by yes or no respectively. As shown in the flowchart, engaging the Emergency Stop button closes both solenoids valves, preventing air from flowing to the turbine even if the manual valve is open. Depressing the Autonomous Operation button tells the controller to begin running the autonomous control algorithm.

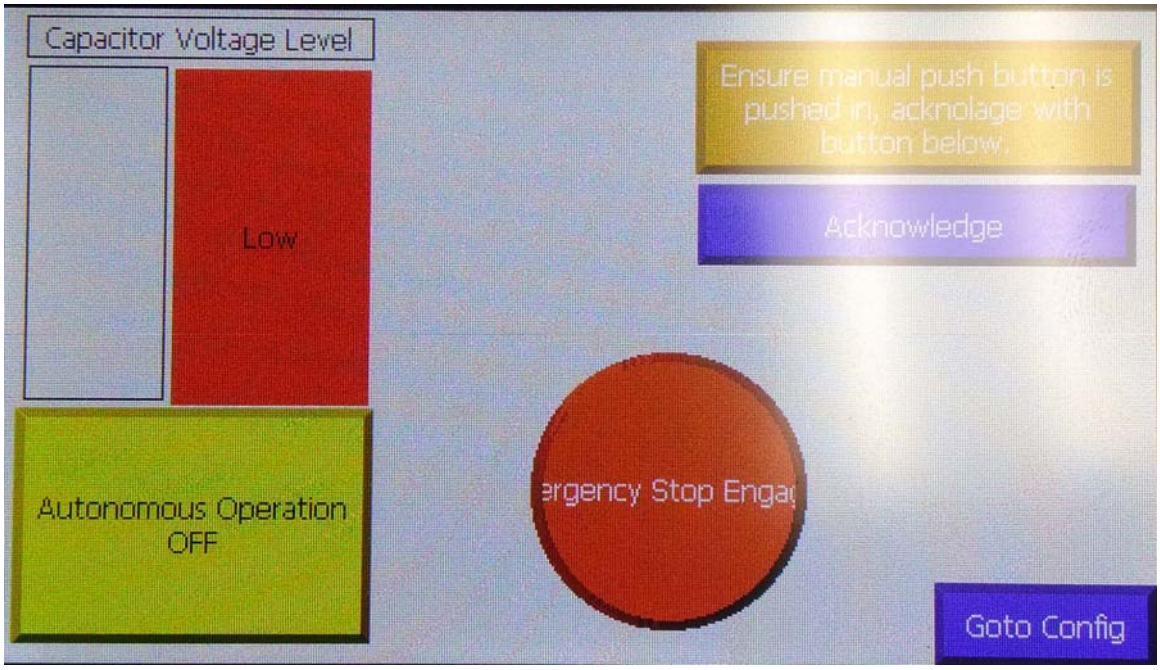

Figure 29 HMI with Emergency Stop Engaged

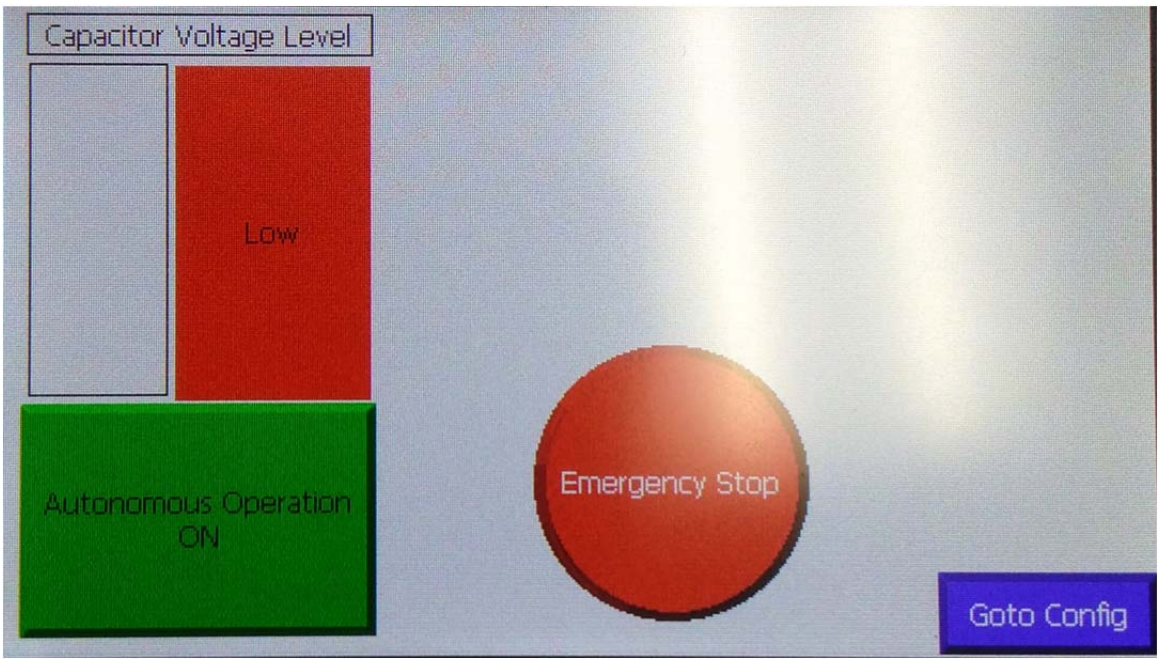

Figure 30 HMI with Autonomous Operation Engaged

3. Autonomous Control Program

Following engagement of the Autonomous Operation button, the autonomous control program will begin to run. The first thing the program does is close the manual side solenoid valve, which eliminates the possibility of the manual valve bypassing the automatic control solenoid valve. Then, the program checks if this is the first time the program has run since receiving power. If it is the first run of the program, a warning banner and acknowledgment button displays on the HMI, which tells the operator to ensure the manual valve is closed. The message is in the upper right of the display, shown in Figure 31. The warning will continue to display until acknowledged by depressing the button. As long as the Micro850 receives power, the warning will not display again and the manual side solenoid valve will remain closed. Even when autonomous run is off, the manual side solenoid valve will remain closed: only when the Micro850 is unpowered will the manual side solenoid valve open.

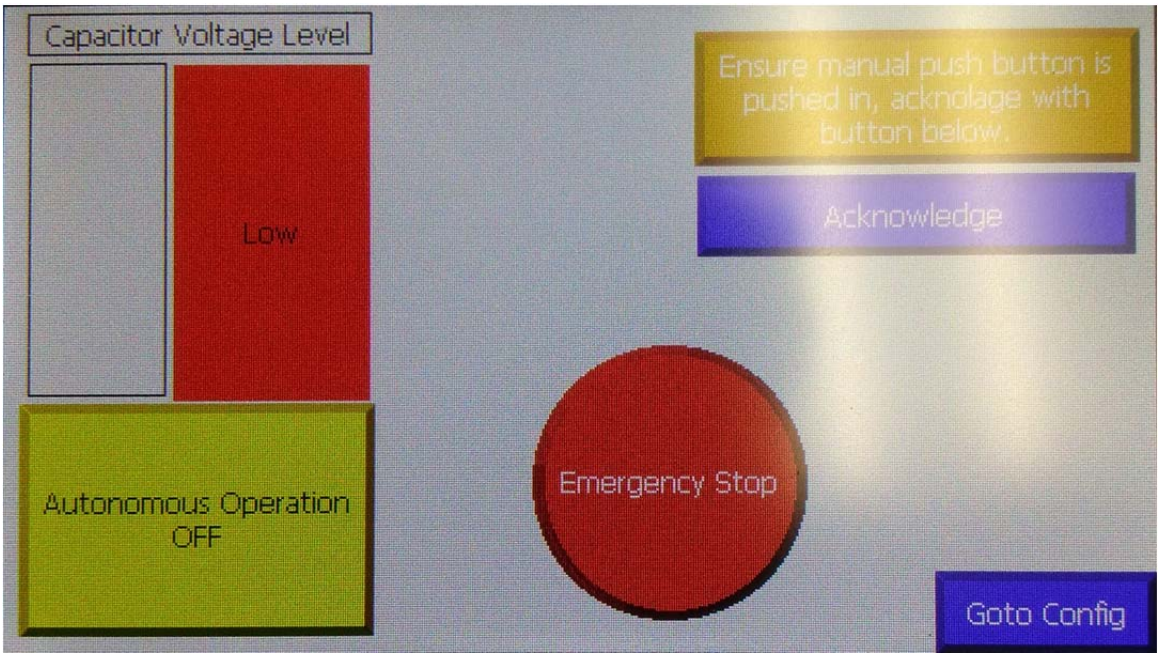

Figure 31 HMI with Warning Displayed

The heart of the control program is the control of the automatic side solenoid valve. A comparison of the capacitor voltage to the established upper and lower bounds

determines the appropriate state of the valve. The program first compares the capacitor voltage to the lower bound value. If capacitor voltage is less than the lower bound, the controller sends a signal to open the automatic side solenoid valve. This allows stored compressed air to spin the turbine connected to the generator to produce electrical power to charge up the capacitor. Once charging begins the program stops comparing the capacitor voltage to the lower bound, instead comparison to the upper bound governs further charging operation. The automatic side solenoid valve will remain open until the capacitor voltage is greater or equal to the upper bound value. Once the voltages are equal, the signal to the automatic side solenoid's relay will cease and the valve will close. In addition, after completely charging the capacitor the program will go back to comparing the capacitor voltage to the lower bound value.

The use of upper and lower bounds prevents continuous cycling of the equipment. Comparison to only one value would result in the capacitor fully charging then the control valve continuously opening and closing to maintain the charge at that one value. Using bounds for comparison allows charging the capacitor completely then discharging over a fixed range, then recharging fully and so on. This reduces the amount of starting stresses experienced by the components.

The program will stop immediately if the Autonomous Operation button is disengaged or the Emergency Stop button is depressed. The Micro850 continuously cycles through all the sub-programs installed. The order of a particular sub-program in the stack establishes its hierarchy. The second highest of the sub-programs' hierarchy is the emergency stop sub-program, with the first being the program that resets the variables during power up. Once one loop of a sub-program is completed the Micro850 jumps to the next sub-program. For example, the autonomous run sub-program compares the voltage once and completes the appropriate action then the Micro850 runs the next sub-program and so on until it cycles back to the autonomous run sub-program. To the user it appears that each sub-program operates continuously, because the total cycle time through all the sub-programs takes milliseconds. Thus, the state of the emergency stop button is checked prior to operating the autonomous sub-program, enabling near instantaneous stoppages.

C. TESTING

CCW does not have a built-in simulation feature. However, it is possible to run the program on the Micro850 and change variable values using CCW. During development of the program, this was a convenient method to check if a part of a program operated as desired. Running a Micro850 while connected to a computer with CCW will display the function block programming with a visual representation of its outputs. Monitoring the output of function blocks of the program while changing the input variables enabled verification of the program operation. Testing the program with this method allowed for quick transition from testing to coding the successive iteration of the control program.

Following the development of a final version, which was a fully functioning program using the CCW testing, testing with the Micro850 disconnected from CCW commenced with the relays and voltage transducer connected to the Micro850. A variable DC voltage power supply, shown in Figure 32, connected to the voltage transducer inputs simulates the SS-CEAS system capacitor. The testing involved changing the voltage output from the power supply. The power supply voltage was set at various levels to start the testing and to check if the control operated as expected. The testing monitored the output of the Micro850 using its indicator lights, along with the operation of the relays, leading to position changes of the solenoid valves. With the manual side solenoid valve closed, testing was completed with input voltages set to the following:

1. maximum capacitor voltage, 16 volts
2. between the upper and lower bound values, 13 to 16 volts
3. below the lower bound, less than 13 volts.

In all cases, the automatic side solenoid valve only opened when the voltage was below the lower bound, verifying the control program operated appropriately at various starting voltages. Further testing was completed where the voltage was raised or lowered from the three starting points listed previously. This testing yielded satisfactory results as well.

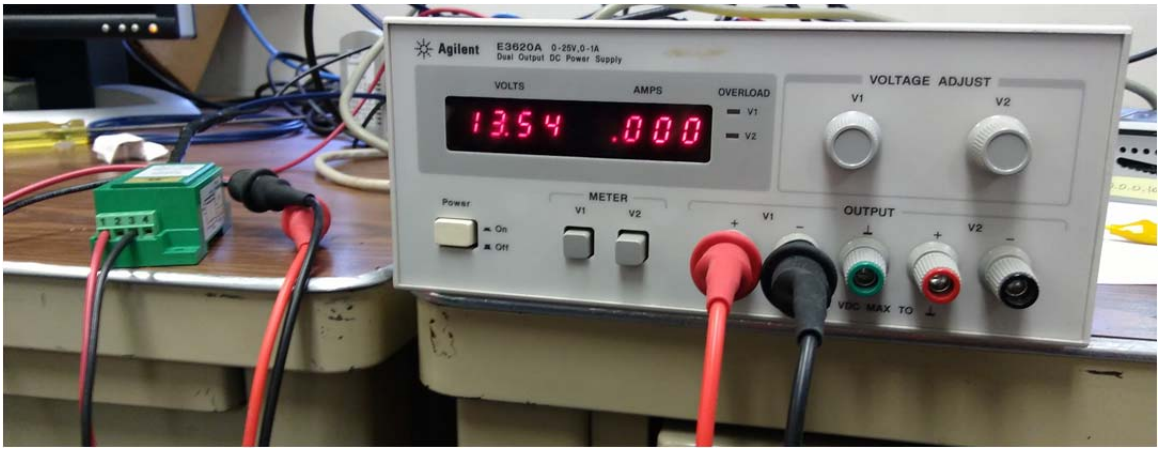

Figure 32 Variable DC Voltage Supply Connected to Voltage Transducer

IV. DARK START ENHANCED SYSTEM ARCHITECTURE

The controller and control program developed will operate as soon as the controller has electrical power. Making a control system that is capable of a dark start requires modifying the power supply. The simplest adaptation of the power supply would be to install an inverter after the capacitor, to create 115V AC to power the components directly from the capacitor. A more advanced design for the modified power system is shown in Figure 33.

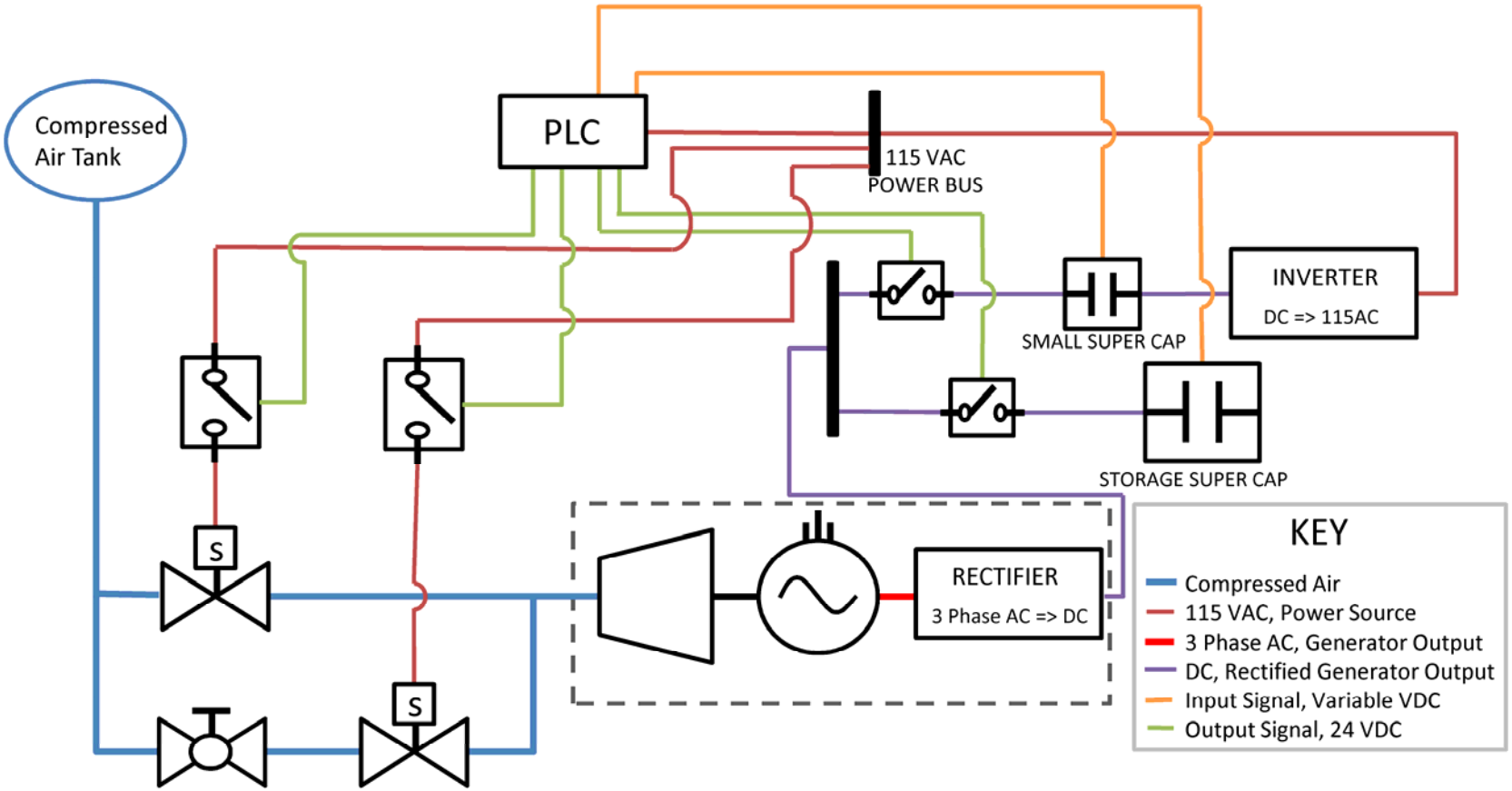

Figure 33 Proposed Modifications to the Power Distribution System

Several new components would be needed to complete this new proposed system including a second smaller capacitor, two additional relays, and an inverter. The power leaving the rectifier that follows the generator would no longer be directly stored on the large storage capacitor. Instead, the rectifier attaches to a bus bar that has two outputs.

One output attached to the rectifier's bus has a normally closed relay followed by a small super capacitor. An inverter takes the DC power from the small super capacitor and converts it to 115V AC. All the powered components such as the Micro 850 and solenoid valves connect to a 115V AC power bus supplied by inverter. This would eliminate the reliance on an external power source. If the SS-CAES system had no power, manually opening the bypass valve would run the generator and charge the small super capacitor. Once the small super capacitor reached sufficient power, the Micro 850 would power on and begin to operate. The Micro 850 would open and close the normally closed relay before the small super capacitor to maintain adequate voltage to operate the control system. Since the relay before the small super capacitor is normally closed, an electromagnetic relay is required.

The second output attached to the rectifier's bus leads to a normally open relay attached to the main storage capacitor. This relay would be closed once the small super capacitor was charged and powering the system. Future iterations of this project may consider having the inverter draw off the storage super capacitor once it was charged. However, that is only possible when the system is in one condition, in which the small super capacitor is already charged. For simplicity, it is proposed that the inverter only draws power from the small super capacitor.

The control program developed already could be easily adapted to integrate these proposed modifications to the power system, which would enable a dark start capable SS-CAES system.

THIS PAGE INTENTIONALLY LEFT BLANK

V. CONCLUSIONS

A control algorithm for a SS-CAES generation system was developed. The control algorithm developed is scalable to a broad range of applications. The control system developed is adequately robust enabling implementation at nearly any DON facility or vessel with preexisting compressed air storage. The use of COTS hardware components enables batch production and scalability of the control system. The control system is dark start capable, only requiring compressed air to generate electrical power. The control system increases the viability of SS-CAES, enabling storage of excess electrical power produced by solar and wind generation.

THIS PAGE INTENTIONALLY LEFT BLANK

VI. RECOMMENDATIONS

Installing an inverter following the capacitor to convert the DC voltage to 115V AC would enable the dark start functionality of the control system. An inverter would power the controller and components directly from the capacitor—meaning no external electrical power would be required. The manual bypass valve would then be used to start the system when there was no charge on the capacitor.

Implementing the system architecture shown in Figure 33 would enhance the dark start functionality. Using a smaller capacity super capacitor to power the inverter, would lead to a decreased delay between manual dark starts and autonomous running.

Installing the SS-CAES system at other DON facilities would require different-sized turbines and generators to match the load requirements and the available compressed air storage. This requires changing the size of the components such as the solenoid valves, manual valves, and piping. The use of piloted solenoids enables the utilization of the same relays used in the proof for all but the largest of applications.

THIS PAGE INTENTIONALLY LEFT BLANK

APPENDIX A. PANELVIEW 800 AND MICRO 850 INTERFACE

The Panelview 800 and Micro 850 have three methods available to interface with each other: serial port, USB port or Ethernet port. For this project, the interface method is the Ethernet ports on the two components. A cross-connect Ethernet cable can link the Panelview 800 and the Micro 850 directly; however, during development, using a Ethernet switch makes reprogramming the components more convenient. The Trednet TEG-S50g Ethernet switch used to interface components is shown in Figure 34. The three connections, shown from left to right, are the cables for the Micro 850, Panelview 800, and computer with CCW installed.

Figure 34 Ethernet Switch Used to Interface Controller and HMI

Configuring the Panelview 800 and Micro 850 to communicate on the Ethernet network requires establishing IP addresses. The IP addresses established are 10.0.0.101 and 10.0.0.100, respectively.

THIS PAGE INTENTIONALLY LEFT BLANK

APPENDIX B. DC VOLTAGE TRANSDUCER

A. HARDWARE

The DC Voltage Transducer requires three connections: input, output, and 24V DC power supply. The device, whose voltage is to be measured, connects to the inputs, shown in Figure 35. The positive wire connects to terminal "1" and the negative wire connects to terminal "3."

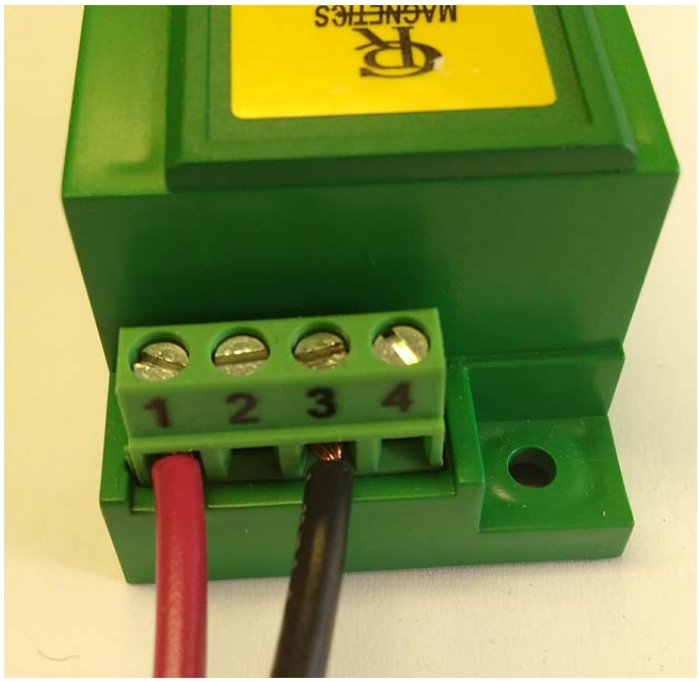

Figure 35 Voltage Transducer Input Terminal

The connections for the output side of the Voltage Transducer are slightly more complicated. The complication is due to the power source and negative output sharing a terminal. To facilitate having a single cable to input to the positive output/power supply terminal the negative output cable and negative power source cable were soldered together. The cable configuration for the 24V DC power source and the output cable is shown in Figure 36. The positive power source cable connects to terminal "5," shown in Figure 36. The negative power source and output connect to terminal "6," shown in

Figure 36. The power source comes from “+CM1” and “-CM1” on the Micro850 output bus, shown in Figure 37. The positive output connects to terminal “8,” shown in Figure 36.

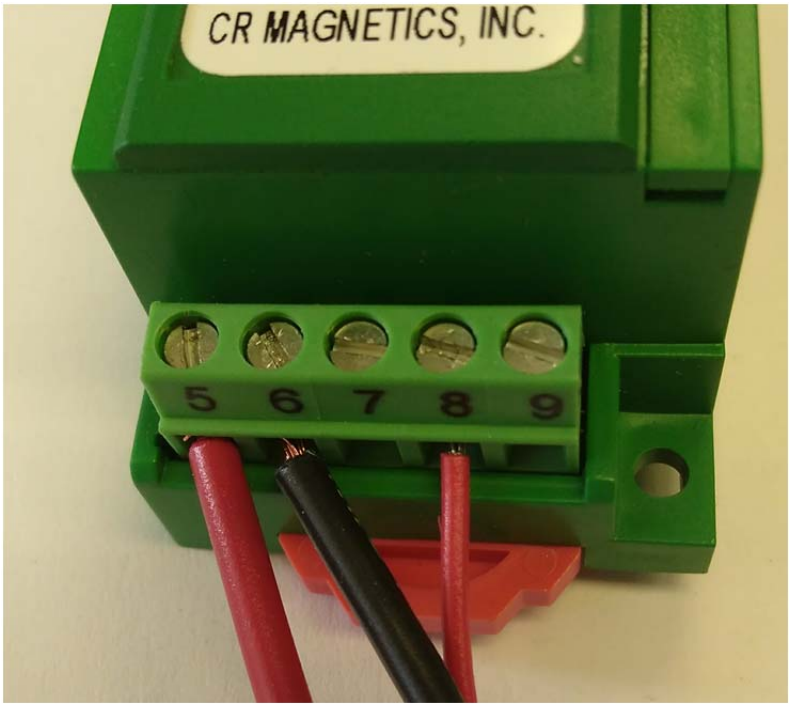

Figure 36 Voltage Transducer Output and Power Source Terminal

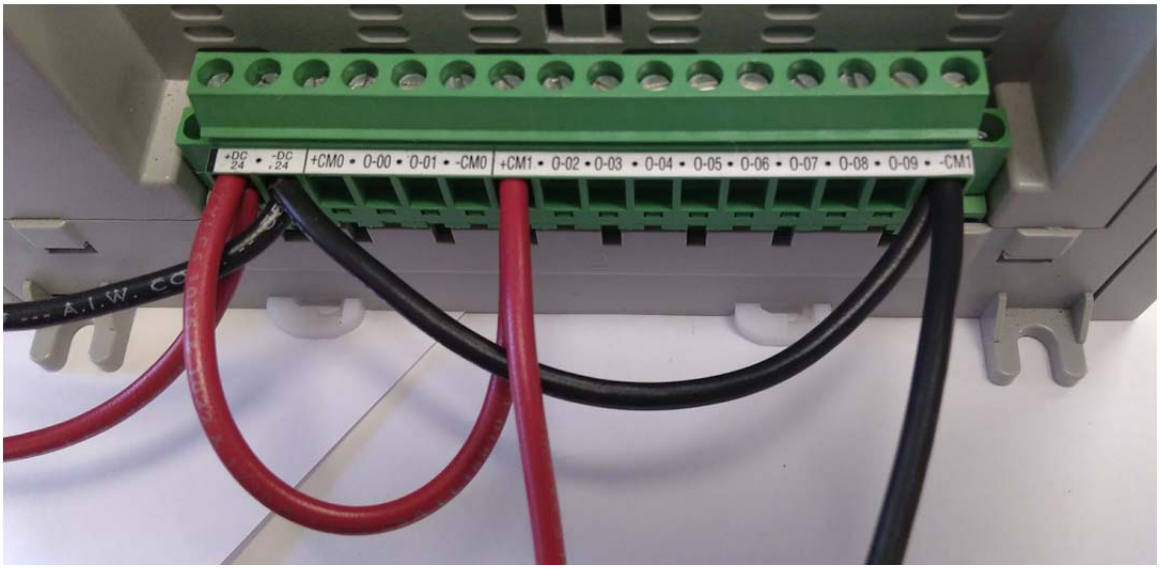

Figure 37 Micro 850 Output Bus

The positive and negative outputs connect to Micro 850 analog module. The positive voltage output from the transducer connects to “VI-0” which is terminal “1,” shown in Figure 38. The negative voltage output from the transducer connects to “COM” which is terminal “3,” shown in Figure 38.

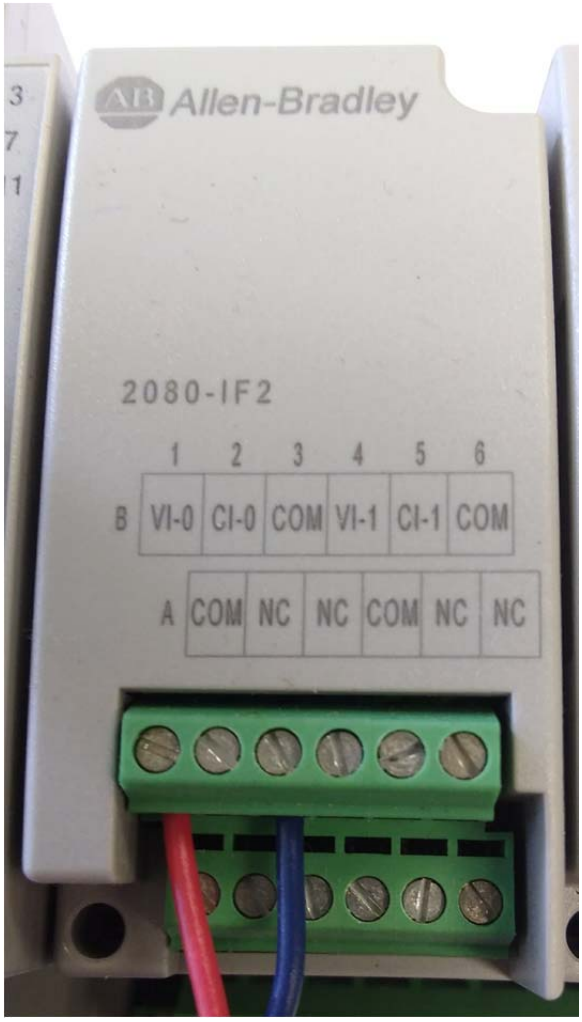

Figure 38 Micro 850 Analog Module

B. SOFTWARE

The input to the analog module establishes a global variable within the Micro 850 programming. The created variable name is *IO_P1_A1_01* and it is an integer data type. Since the voltage is not sensed directly by the analog module; instead, it passes through

the voltage transducer. The signal received by the analog module must be processed within the Micro 850 program to represent voltage. Using a built-in function in CCW called *SCALER*, the input sensed by the analog module is converted to the actual voltage of the capacitor. The sub program used to scale the input is shown in Figure 39.

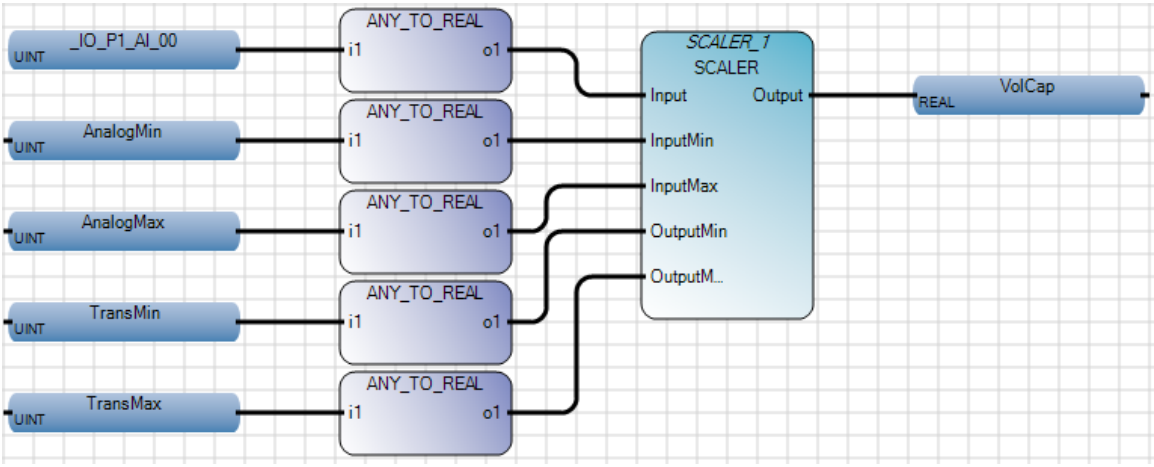

Figure 39 Sub Program to Scale Sensed Voltage to Actual Voltage

The scaler function requires five inputs; the inputs to the function must also be real data type. The first step of this program is to convert all the integer variables to real using the *ANY_TO_REAL* function block. The first input to the scaler function is the input sensed by the analog module. The next two inputs are the minimum and maximum values of the analog module, 0V and 10V respectively. The *AnalogMax* variable value is 65535, which is what the analog module outputs when it senses 10V. The last two inputs are the minimum and maximum values of the voltage transducer, 0V and 75V respectively. Using these inputs, the *SCALER* function outputs the actual value of the voltage of the capacitor. The variable name given to the true capacitor voltage is *VolCap*.

APPENDIX C. RELAY CONNECTION

Relays enable controlling the operation of the solenoid valves using the Micro 850. The supply power to the solenoid valves is interrupted by the relays. The Micro 850 energizes the relays, closing the relay contacts and allowing supply power to flow to the solenoid valves.

The SSR relays used have four connection terminals, shown in Figure 40. The output of the relays is what is connected to the component that is being controlled; in this case the solenoid valves. The output of the relay consists of terminals *1* and *2*, these terminals separate the negative wire of the solenoid power source. The input of the relay is consists of terminals *3* and *4*, these are connect to the output of the Micro 850 were the positive output connects to terminal *3* and the negative output connects to thermal *4*.

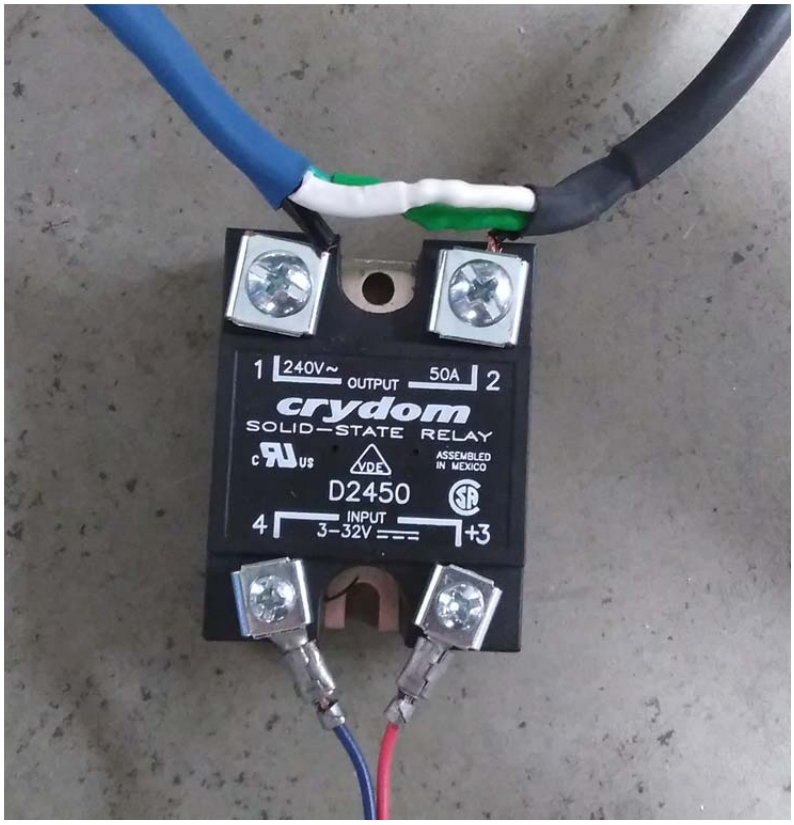

Figure 40 SSR with Solenoid and Micro 850 Attached

THIS PAGE INTENTIONALLY LEFT BLANK

APPENDIX D. SOLENOID VALVE CONNECTIONS

A. ELECTRICAL CONNECTIONS

Actuation of the solenoid valves requires voltage to be applied to the solenoid inside the valve. The source voltage for the solenoids used for this project use 115V AC. The voltage first connects to the power supply then the relay before continuing to the solenoid valves. Appendix C discusses connection between the relay and solenoid valve. The power cable continues from the relay and is attached to a terminal block, shown in Figure 41. Connecting the power cable to this terminal block is strait forward, as the ground, positive, and negative thermals are all labeled.

Figure 41 Solenoid Female Connection

The female terminal block mates to the solenoid's male terminal connection and is affixed using the screw shown in Figure 41. The male terminal on the solenoid has three matching connection posts, shown in Figure 42.

Figure 42 Solenoid Male Connection

B. PNEUMATIC CONNECTIONS

The pneumatic connections for the solenoid valves are identical whether they are normally open or normally closed valves. There are three ports on the valves as shown by the label on the valve in Figure 43. The input is always connected to port *1* and the output is connected to port *2*. The position of the ports changed based on whether the valve is normally open or closed but the connection numbering remains consistent. Port *3* is an exhaust port for all applications; in this project, it is not required and was plugged.

Figure 43 Solenoid Valve Port Label

THIS PAGE INTENTIONALLY LEFT BLANK

APPENDIX E. MICRO850 VARIABLES

The Micro850 has two types of variables, global and program. The key difference between the two variable types is their persistence following a loss of power to the controller. The state of the global variables persists by using the internal flash memory of the Micro850 to store their state in the event of the Micro850 losing power. The program variables, on the other hand, are stored on the RAM of the Micro850, so when the Micro850 loses power the program variables values are lost.

A. GLOBAL

The global variable list is shown in Figure 44 and Figure 45. The variable names in gray are prebuilt variables in the Micro 850 and the variable names in white are programmer created variables.

Name	Alias	Data Type	Dimension	Project Value	Initial Value
_IO_EM_DO_00		BOOL		FALSE	
_IO_EM_DO_01		BOOL		TRUE	
_IO_EM_DO_02	Auto Sol	BOOL		FALSE	
_IO_EM_DO_03	Man Sol	BOOL		FALSE	
_IO_EM_DO_04		BOOL		FALSE	
_IO_EM_DO_05		BOOL		FALSE	
_IO_EM_DO_06		BOOL		FALSE	
_IO_EM_DO_07		BOOL		FALSE	
_IO_EM_DO_08		BOOL		FALSE	
_IO_EM_DO_09		BOOL		FALSE	
_IO_EM_DI_00		BOOL		FALSE	
_IO_EM_DI_01		BOOL		FALSE	
_IO_EM_DI_02		BOOL		FALSE	
_IO_EM_DI_03		BOOL		FALSE	
_IO_EM_DI_04		BOOL		FALSE	
_IO_EM_DI_05		BOOL		FALSE	
_IO_EM_DI_06		BOOL		FALSE	
_IO_EM_DI_07		BOOL		FALSE	
_IO_EM_DI_08		BOOL		FALSE	
_IO_EM_DI_09		BOOL		FALSE	
_IO_EM_DI_10		BOOL		FALSE	
_IO_EM_DI_11		BOOL		FALSE	
_IO_EM_DI_12		BOOL		FALSE	
_IO_EM_DI_13		BOOL		FALSE	
_IO_P1_AI_01		UINT		0	
PushAch		BOOL		TRUE	0
PushAlert		BOOL		FALSE	0
BabyGood		BOOL		FALSE	0
PushAlertString		STRING		'Ensure manual	'Ensure manual push button is pushed in, acknolage with butt
AUTOONOFF		BOOL		FALSE	0
EStop		BOOL		FALSE	0
AnalogMin		UINT			0

Figure 44 Global Variable List Part 1

Name	Alias	Data Type	Dimension	Project Value	Initial Value	Comment
AnalogMax		UINT			65535	
TransMin		UINT			0	
TransMax		UINT			75	
VolCap		REAL				
VolCapUp		REAL			16.0	
VolCapLow		REAL			13.0	
ChargeInd		BOOL				
Chargestat		BOOL				
CapInBrkt		BOOL				
VolCapInt		INT				
__SYSVA_ABORT_CYCLE		BOOL		FALSE	FALSE	Aborting Cycle
_IO_P1_AI_00		UINT		13		Baby Cap Voltage
__SYSVA_TCYCURRENT		TIME		T#1ms		Current cycle time
__SYSVA_CYCLECNT		DINT		1754209		Cycle counter
__SYSVA_CCEXEC		BOOL		FALSE		Execute one cycle when applicatio
__SYSVA_FIRST_SCAN		BOOL		FALSE	TRUE	First scan bit
__SYSVA_SCANCNT		DINT		1754225		Input scan counter
__SYSVA_KVBCERR		BOOL		FALSE		Kernel variable binding consuming
__SYSVA_KVBPERR		BOOL		FALSE		Kernel variable binding producing
__SYSVA_SUSPEND_ID		UINT		0	0	Last Suspend ID
__SYSVA_MAJ_ERR_HALT		BOOL		FALSE	FALSE	Major Error Halted status
__SYSVA_TCYMAXIMUM		TIME		T#4ms		Maximum cycle time since last star
__SYSVA_TCYOVERFLOW		DINT		0		Number of cycle overflows
__SYSVA_POWERUP_BIT		BOOL		FALSE	TRUE	Power-up bit
__SYSVA_TCYCYCTIME		TIME		T#0s		Programmed cycle time
__SYSVA_PROJ_INCOMPL		UDINT		0	0	Project Incomplete
__SYSVA_REMOTE		BOOL		TRUE	FALSE	Remote status
__SYSVA_RESMODE		SINT		3		Resource execution mode
__SYSVA_RESNAME		STRING		'CONTROLLER\		Resource name (max length=255)
__SYSVA_TCYWDG		UDINT		2000	2000	Software Watchdog
__SYSVA_CYCLEDATE		TIME		T#15m19s713n		Timestamp of the beginning of the
__SYSVA_USER_DATA_LOS		BOOL		FALSE	FALSE	User data lost

Figure 45 Global Variable List Part 2

B. PROGRAM

The program variables, none of the variables are grey because all program variables are created by the programmer are shown in Figure 46.

Name	Alias	Data Type	Dimension	Project Value	Initial Value
VBabyCap		UINT		0	0
Count		INT		0	0
CUOne		DINT		1	1
TP_1		TP		...	...
POLETIME		TIME		T#10s	T#10s
DINT_0		DINT		0	0
Dummy		BOOL		FALSE	0
OH		BOOL		FALSE	0
one		BOOL		TRUE	1
CTU_2		CTU		...	...
DINT_2		DINT		2	2
Cont_On		BOOL		FALSE	0
BabyCapMax		UINT		15	15
DINT_1		DINT		1	1
TON_1		TON		...	...
SwitchTime		TIME		T#4s	T#4s
RelayA		BOOL		FALSE	0
RelayB		BOOL		TRUE	0

Figure 46 Program Variable List

THIS PAGE INTENTIONALLY LEFT BLANK

APPENDIX F. SUPPORTING PROGRAMS

A. RESTING GLOBAL VARIABLES

Since the global variables are stored even when the Micro 850 loses power, resting global variables to desired initial values is required every time the Micro 850 is initially supplied power. The sub program developed to reset global variables when the Micro850 initially receives power is shown in Figure 47. The program makes use of a built-in variable of the Micro 850 *SYSVA_POWER_BIT*, which is *true* initially when the Micro850 receives power then shifts to *false* once one cycle of the program finishes. The program uses *NOT* function blocks that check if the input is not *true*. So when the input is *false* it returns *true* when the input is *true* it returns *false*.

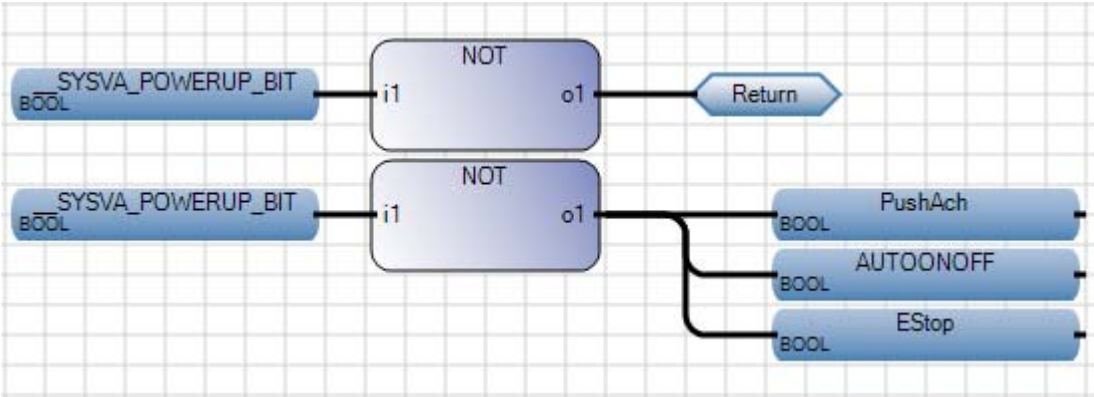

Figure 47 Global Variable Reset Sub Program

The first *NOT* block makes sure the values are only changed if this is the initial power on. When first powered on the input to the *NOT* block is *true* so the output is *false*, so the return will not execute. Then, once the *SYSVA_POWER_BIT* flips to *false* the *NOT* block will return *true*, executing the return, which leaves the program.

The second *NOT* block is only reached when the first *NOT* block does not execute the return. Thus, only when the input variable *SYSVA_POWERUP_BIT* is *true* the second *NOT* block makes the global variables *false.* When *SYSVA_POWERUP_BIT* is *false* the second *NOT* block is not reached and the global variables are unchanged. Meaning the

values of three global variables only change when the Micro 850 initially receives powered:

1. *PushAch*, which is the acknowledgement for the manual valve warning
2. *AUTOONOFF*, which is the toggle for autonomous operation
3. *EStop*, which is the toggle for the emergency stop

B. EMERGENCY STOP

The emergency stop program enables the user to stop the operation of the generator immediately. The sub program developed for the emergency stop is shown in Figure 48. The emergency stop program makes use of *NOT* function blocks in a similar manner to the global variable rest program.

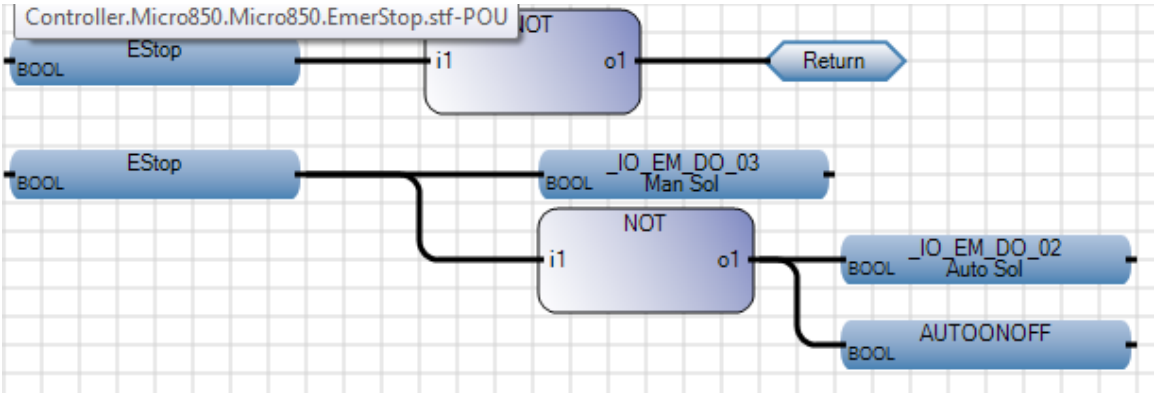

Figure 48 Emergency Stop Sub Program

The first not blocks executes the return and leave the sub program until the Estop variable becomes *true* after the button on the HMI has been depressed. Once the Estop variable becomes *true*, the rest of the sub program executes, simply changing the values of three variables. The second not block is used to invert the "true" from the Estop variable to allow for two of the variables to be made "false." When the Estop variable is *true*, the three variables changed are:

4. *IO_EM_DO_03*, goes to *true*, which is connected to the manual solenoid relay, thus closing the contact in the relay which closes the manual solenoid valve

5. *IO_EM_DO_02*, goes to *false*, which is connected to the automatic solenoid relay, thus opening the contact in the relay which closes the automatic solenoid valve

6. *AUTOONOFF*, goes to *false*, disabling the autonomous operation program

C. HMI STATUSES

The HMI uses programs on the Micro 850 to display any status. The HMI, the buttons and status indicator, is associated with variables on the Micro 850. In addition, the HMI can only read Boolean and integer variables. The two status indicators on the HMI require sub programs to create variables that are readable by the HMI.

The status indicator of the capacitor voltage on the HMI uses the program in Figure 49. The status is associated with the Boolean variable *BabyGood*, which is created by the comparison of the voltage of the capacitor, *VolCap*, and the lower bound of the capacitor voltage, *VolCapLow*. When *BabyGood* is *true*, the status is green and shows "Good." When *BabyGood* is *false*, the status is yellow and shows "Low."

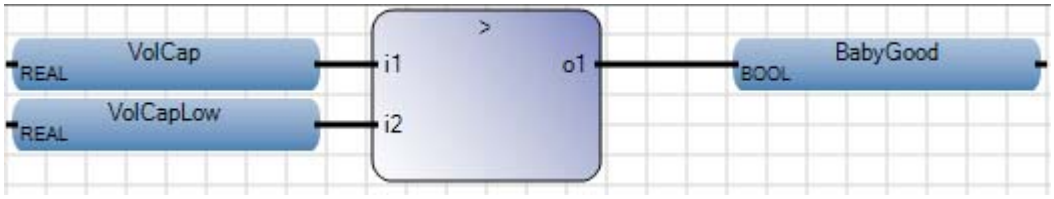

Figure 49 Sub Program for Voltage Status Indicator

The bar scale on the HMI that shows the charge level of the capacitor using an integer input. When setting up the bar scale, a maximum value is input to determine the scale of the bar. The measured voltage of the capacitor, *VolCap*, is a real data type; the HMI bar scale requires integer data types. The sub program that uses *ANY_TO_INT* to convert, *VolCap*, a real data type to, *VolCapInt*, an integer data type is shown in Figure 50.

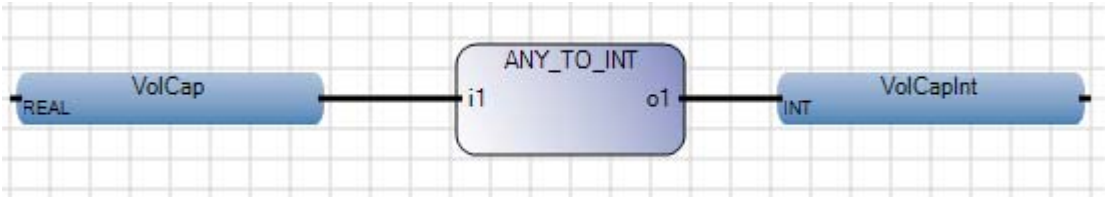

Figure 50 Sub Program for Voltage Level Bar Indicator

APPENDIX G. CONTROL PROGRAMS

A. BOUNDARY CHECKING PROGRAM

The first step in the control program is checking if the capacitor voltage, *VolCap*, is within the acceptable bounds for the capacitor voltage. The sub program developed to check the voltage against the boundaries is shown in Figure 51. The main component of the program is the *RS* function block, which is a bistable reset/set function block. *CapInBrkt* indicates if the voltage is within the boundaries, when it is within the boundary it has a value of *true* otherwise it is *false*. The initial value of *CapInBrkt* is *false*.

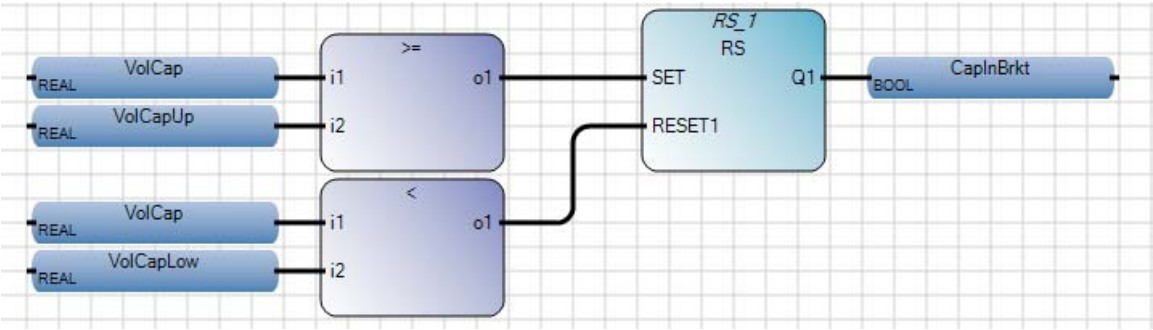

Figure 51 Boundary Checking Sub Program

The program first checks if the capacitor voltage, *VolCap*, is greater than or equal to the upper bound of the acceptable voltage, *VolCapUp*. *CapInBrkt* will remain *false* until *VolCap* is greater than or equal to *VolCapUp*. Due to the *RS* block once *CapInBrkt* becomes *true* it will remain *true* until the *RS* block is reset, even when *VolCap* is less than *VolCapUp*. The *RS* block is reset by the second comparison block. When *VolCap* is less than the lower bound of the acceptable voltage, *VolCapLow*, *true* is input to *RESET1* resetting the *RS* block making *CapInBrkt false*.

B. MAIN CONTROL PROGRAM

The program developed for autonomous operation is shown in Figure 52.

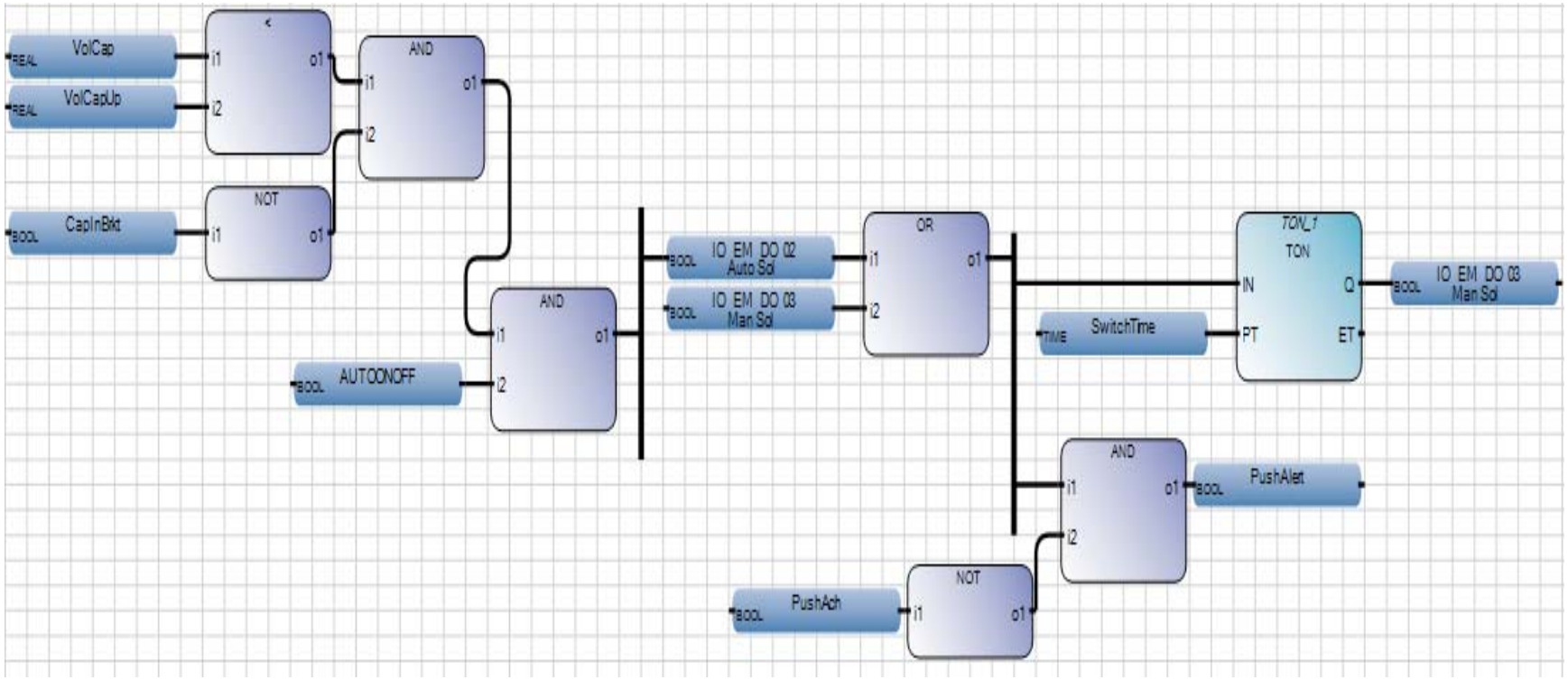

Figure 52 Autonomous Operation Sub Program

The first step of the autonomous operation sub program is to check if *VolCap* is less than *VolCapUp*, which prevents over charging the capacitor. If *VolCap* is less than *VolCapUp true* is output. This output is fed into one input of an *AND* function block, the second input receives the inverted valve of *CapInBrkt* from the boundary sub program. An *AND* function block will only output *true* when both inputs are also *true*. Meaning, only when the *VolCap* is less than *VolCapUp* and *CapInBrkt* is *false* the *AND* block will output *true*. Since the *CapInBrkt* variable begins with a value of *false* the first time the autonomous program runs this *AND* block will return *true* even if the voltage of the capacitor is within the bounds as long as *VolCap* is less than *VolCapUp*. This means that at start up the program will charge the capacitor to its maximum voltage even if the capacitor voltage is only slightly below the maximum voltage. In addition, due to the boundary checking program, all subsequent charging of the capacitor will begin once the voltage falls below the lower bound; the charge process then will continue until the capacitor reaches its maximum charge level.

The output from the first *AND* block is connected to the input of a second *AND* block the other input is the *AUTOONOFF* variable which is controlled by the HMI. When the *AUTOONOFF* button is depressed and the first *AND* block determines charging is appropriate the second *AND* block outputs *true*. This makes *IO_EM_DO_02 true* closing the automatic relay, which opens the automatic solenoid. This passes air over the turbine to spin the generator and charge the capacitor.

The next function block is an *OR* with two inputs *IO_EM_DO_02* and *IO_EM_DO_03*, which are the automatic and manual relay outputs, respectively. If either of the inputs to this function block is *true*, the output is *true*. The output of this *OR* block goes to a bus bar from which branch two program segments.

The first, top, segment off the OR bus bar uses a TON function block. This block is a time delay operator, when the input is *true* the output changes to *true* after the time specified by the time variable input, in this case, *SwitchTime*, 3 seconds. After the delay, *IO_EM_DO_03* is set to *true* which closes the manual solenoid valve. Due to the previous *OR* block, once *IO_EM_DO_03* is set to *true* it will remain true until the Micro

850 loses power. Meaning, the manual solenoid valve will close once autonomous operation begins and remain closed until the Micro 850 is cut off from its power source.

The second, bottom, segment off the *OR* bus bar is the segment of the program that initiates the warning to ensure the manual valve is closed. There is an *AND* block that has one input from the bus bar and a second input which is the inverted value of the acknowledgement push button, *PushAch*. Only when both inputs are *true* the *AND* block will output *true* displaying the warning, *PushAlert*, and acknowledgment button. Once the user depresses the acknowledgement button, *PushAch* will be set to *true* which will make the *AND* block out put *false* and *PushAlert* will remain false until the power source is removed from the Micro850.

APPENDIX H. HIERARCHY OF PROGRAMS

The hierarchy of programs determines the order of precedence of the sub programs. The hierarchy of the sub programs is shown in Figure 53. The Micro 850 runs the programs from top to bottom.

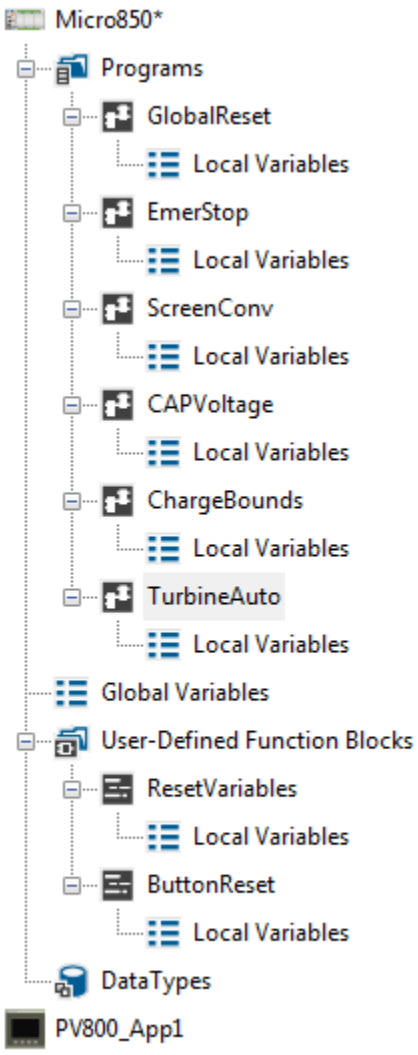

Figure 53 Program Hierarchy

THIS PAGE INTENTIONALLY LEFT BLANK

LIST OF REFERENCES

[1] Department of the Navy, 2010, "Department of the Navy's Energy Program for Security and Independence," Washington, DC, http://www.secnav.navy.mil/eie/ASN%20EIE%20Policy/Naval_Energy_Strategic_Roadmap.pdf

[2] McGinn, D., 2016, "Microgrids: Macro Benefits for Our Navy Bases," http://navylive.dodlive.mil/2016/05/02/microgrids-macro-benefits-for-our-navy-bases/

[3] Office of the Assistant Secretary of Defense, 2015, "Department of Defense Annual Energy Management Report Fiscal Year 2014," Washington, DC, http://www.acq.osd.mil/eie/Downloads/Reports/Tab%20B%20-%20FY%202014%20AEMR_FINAL.pdf

[4] Department of Defense, 2015, "Department of Defense 2016 Operation Energy Strategy," 5-240277A, Washington, DC, http://www.acq.osd.mil/eie/Downloads/OE/2016%20DoD%20Operational%20Energy%20Strategy%20WEBc.pdf

[5] Spector, J., 2016 "From Solar to Second-Life Batteries: Why the Navy Leads the U.S. Government in clean energy deployment," https://www.greentechmedia.com/articles/read/navy-leads-federal-government-in-clean-energy-solar-storage

[6] UniEnergy Technologies, 2016, "U.S. Navy Selects UET to Provide Energy Storage-based Resiliency for Naval Base Ventura County" http://www.uetechnologies.com/news/84-nb-ventura

[7] Zhoa, H., Li, W., Taft, C., and Bentsman, J., 1999, "Robust Controller Design for Simultaneous Control of Throttle Pressure and Megawatt Output in a Power Plant Unit," *IEEE International Conference on Control Applications*, Institute of Electrical and Electronics Engineers, Kohala Coast, HI., pp. 802–807.

[8] Ellabban, O., Haitham, A.-R., and Blaabjerg, F., 2014, "Renewable Energy Resources: Current Status, Future Prospects and Their Enabling Technology," *Renewable and Sustainable Energy Reviews*, **39**, pp. 748–764.

[9] Zervos, A., Lins, C. and Muth, J., 2010, "RE-thinking 2050 a 100% Renewable Energy Vision for the European Union," European Renewable Energy Council, Brussels, Belgium, pp. 1–76.

[10] Jewell, W., and Ramakumar, R., 1987, "The Effects of Moving Clouds on Electric Utilities with Dispersed Photovoltaic Generation," *IEEE Transactions on Energy Conversion*, **EC-2**(4), pp. 570–576.

[11] Kaldellis, J., and Kokala, A., 2010, "Quantifying the Decrease of the Photovoltaic Panels Energy Yield Due to Phenomena of Natural Air Pollution Disposal," *Energy*, **35**(12), pp. 4862–4869.

[12] Paatero, J., 2005, "Effect of Energy Storage on Variations in Wind Power," *Wind Energy*, **8**(4), pp. 421–441.

[13] Bryden, I., 2006, "ME1—Marine Energy Extraction: Tidal Resource Analysis," *Renewable Energy*, **31**(2), pp. 133–139.

[14] Sheu, E., Mitsos, A., Eter, A., Mokheimer, E., Habib, M., and Al-Qutub, A., 2012, "A Review of Hybrid Solar–Fossil Fuel Power Generation Systems and Performance Metrics," *Journal of Solar Energy Engineering*, **134**(4), pp. 041006 1–17.

[15] Chen, H., Cong, T., Yang, W.,Tan, C., Li, Y., and Ding, Y., 2009, "Progress in Electrical Energy Storage System: A Critical Review," *Progress in Natural Science*, **19**, pp. 291–312.

[16] International Electrotechnical Commission, 2011, "Electrical Energy Storage White Paper," *Geneva, Switzerland: International Electrotechnical Commission*, Geneva, Switzerland, pp. 1–78.

[17] Bradbury, K., 2010 "Energy Storage Technology Review," Duke University, pp. 1–34.

[18] Barnes, F., and Levine, J., 2011, *Large Energy Storage Systems Handbook*, Taylor & Francis Group, Boca Raton, FL., p. 254.

[19] Kucukali, S., 2014, "Finding the Most Suitable Existing Hydropower Reservoirs for the Development of Pumped-Storage Schemes: An Integrated Approach," *Renewable and Sustainable Energy Reviews*, **37**, pp. 502–508.

[20] Pimm, A., Garvey, S., and Jong, M., 2014 "Design and Testing of Energy Bags for Underwater Compressed Air Energy Storage," *Energy*, **66**, pp. 496–508.

[21] Jong, M., 2014, "Commercial Grid Scaling of Energy Bags for Underwater Compressed Air Energy Storage," *Offshore Energy & Storage Symposium*, Windsor, Canada, pp. 1–5.

[22] Bolund, B., Bernhoff, H., and Leijon, M., 2007, "Flywheel Energy and Power Storage System," *Renewable & Sustainable Energy Reviews*, **11**, pp. 235–258.

[23] Ahrens, M., Kucera, L., and Larsonneur, R., 1996, "Performance of a Magnetically Suspended Flywheel Energy Storage Device," *IEEE Transactions on Control Systems Technology*, **4**(5), pp. 494–502.

[24] P. E. Staff, 2013, "Beacon Begins Operation of New Flywheel Energy Storage Plant in Pennsylvania," http://www.pennenergy.com/articles/pennenergy/2013/09/beacon-begins-operation-of-new-energy-storage-system-in-pennsylvania.html

[25] Soloveichik, G., 2011, "Battery Technologies for Large-Scale Stationary Energy Storage," The Annual Review of Chemical and Biomolecular Engineering, **2**, pp. 503–529.

[26] UAF Staff, 2012, "Light Inspects ACEP's Battery Bank," https://news.uaf.edu/light-inspects-aceps-battery-bank/

[27] Areans, L., Walsh, F., and Ponce de Leon, C., 2015 "3D-Printing of Redox Flow Batteries for Energy Storage: A Rapid Prototype Laboratory Cell," ECS Journal of Solid State Science and Technology, **4**, pp. 3080–3085.

[28] Larcher, D., and Tarascon, J., 2015 "Towards Greener and More Sustainable Batteries for Electrical Energy Storage," *Nature Chemistry*, **7**, pp. 19–30.

[29] Palomares, V., Serras, P., Villaluenga, I., Hueso, K., Carretero-Gonzalez, J., and Rojo, T., 2012, "Na-ion Batteries, Recent Advances and Present Challenges to Become Low Cost Energy Storage Systems," *Energy & Environmental Science*, **5**, pp. 5884–5901.

[30] Soloveichik, G. L., 2015, "Flow Batteries: Current Status and Trends," *Chemical Reviews,* **115**(20), pp. 11533–11558.

[31] Zhang, W. J., 2011, "A Review of the Electrochemical Performance of Alloy Anodes for Lithium-ion Batteries," *Journal of Power Sources,* **196**(1), pp. 13–24.

[32] Crotogino, F., Donadei, S., Bunger, U., and Landinger, H., 2010, "Large-Scale Hydrogen Underground Storage for Securing Future Energy Supplies," *Proceedings of 18th World Hydrogen Energy Conference (WHEC2010)*, Essen, Germany, pp. 37–45.

[33] Chiesa, P., Lozza, G., and Mazzocchi, L., 2003, "Using Hydrogen as Gas Turbine Fuel," *ASME Turbo Expo 2003, collocated with the 2003 International Joint Power Generation Conference*, American Society of Mechanical Engineers, Atlanta, Georgia, **3**, pp. 163–171.

[34] Ozarslan, A., 2012 "Large-Scale Hydrogen Energy Storage in Salt Caverns," *International Journal of Hydrogen Energy*, **37**(19), pp. 14265–14277.

[35] Energy Infrastructure, 2017, “Underground Natural Gas Storage,” http://www.energyinfrastructure.org/energy-101/natural-gas-storage

[36] Hoffmann, C., and Bremen, L., 2009, “Storage and Transport Capacities in Europe for a Full Renewable Power Supply System,” *14. Kassel Symposium Energy Systemstechnik*, Kassel, Germany, p. 36.

[37] TDK Corporation, 2017, “Principle and Construction of Electric Double Layer Capacitor (EDLC),” http://www.global.tdk.com/techmag/electronics_primer/vol8.htm

[38] WTEC, 1997, “Chapter 2: Magnetic Energy Storage Efforts in Japan,” http://www.wtec.org/loyola/scpa/02_06.htm

[39] Hasnain, S., 1998, “Review on Sustainable Thermal Energy Storage Technologies, Part I: Heat Storage Materials and Techniques,” *Energy Conversion and Management*, **39**(11), pp. 1127–1138.

[40] Zalba, B., Marin, J., Cabeza, L., and Mehling, H., 2003, “Review on Thermal Energy Storage with Pphase Change: Materials, Heat Transfer Analysis and Applications,” *Applied Thermal Engineering*, **23**, pp. 251–283.

[41] Hermann, U., Kelly, B., and Price, H., 2004, “Two-tank Molten Salt Storage for Parabolic Trough Solar Power Plants,” *Energy*, **29**(5–6), pp. 883–893.

[42] Olewitz, C., 2016, “Take a Peek Inside Nevada’s New Solar Farm that Generates Power 24/7 with Molten Salt,” https://www.digitaltrends.com/cool-tech/peek-inside-nevada-solar-plant-247-power-molten-salt/

[43] Department of the Navy, 2015, “Naval Station Newport—Leaning Forward to Meet the Future,” https://www.cnic.navy.mil/regions/cnrma/installations/ns_newport/om/environmental_support/energy.html

[44] Oudalov, A., Cherkaoui, R., and Beguin, A., 2007, “Sizing and Optimal Operation of Battery Energy Storage System for Peak Shaving Application,” *In Power Tech*, Institute of Electrical and Electronics Engineers, Lausanne, Switzerland, pp. 621–625.

[45] Prinsen, T. H., 2016, “Design and Analysis of a Solar-Powered Compressed Air Energy Storage System,” MSME thesis, Naval Postgraduate School, Monterey, CA.

[46] Williams, J., 2017, “Automated Control of a Solar Microgrid Powered Air Compressor for Use in a Small-Scale Compressed Air Energy Storage System,” MSME thesis, Naval Postgraduate School, Monterey, CA.

[47] McLaughlin, C. S., 2016, “Small-Scale Air-Driven Generator,” MSME thesis, Naval Postgraduate School, Monterey, CA.

[48] Allen-Bradley, 2013, “Micro800 Programmable Controller Family,” Bulletin 2080, Rockwell Automation, pp. 1–64, http://literature.rockwellautomation.com/idc/groups/literature/documents/sg/2080-sg001_-en-p.pdf

[49] Allen-Bradley, 2015, “Micro800 Plug-in Modules,” Rockwell Automation, pp. 1–118, http://literature.rockwellautomation.com/idc/groups/literature/documents/um/2080-um004_-en-e.pdf

[50] Parker, 2017, “Solenoid Fluid Control Valves,” http://ph.parker.com/us/en/solenoid-fluid-control-valves

[51] Parker, 2017, “Pneumatic Solenoid Valve - B6 Series,” http://ph.parker.com/us/en/pneumatic-solenoid-valve-b6-series

[52] Agarwal., T., 2015, “Different Types of Relays and their Working Principles,” https://www.elprocus.com/different-types-of-relays-used-in-protection-system-and-their-workings/

[53] Cyrdom, 2016, “Series 1 240V AC Datasheet,” Rev. 040816, pp. 1–8, http://www.crydom.com/en/products/catalog/series-1-240-ac-panel-mount.pdf

[54] Omron, 2014, “G7S-[]-E,” http://www.ia.omron.com/products/family/1446/specification.html

[55] CR Magnetics, 2017, “CR5311 DC Voltage Transducer—0-10V DC Output,” http://www.crmagnetics.com/dc-voltage-transducers/cr5311

[56] Maxwell, 2017, “16V Modules Datasheet,” 1009363.10, pp. 1-5, http://www.maxwell.com/images/documents/datasheet_16v_module.pdf

[57] Leising, R. A., Palazzo, M. J., Takeuchi, E. S., and Takeuchi, K. J., 2001, “Abuse Testing of Lithium-Ion Batteries: Characterization of the Overcharge Reaction of LiCoO2/Graphite Cells,” *Journal of The Electrochemical Society*, 148(8), pp. A838–A844.

[58] Basu, S., and Undeland, T. M., 2008, “A Novel Design Scheme for Improving Ultra-Capacitor Lifetime While Charging with Switch Mode Converters,” *In Power Electronics Specialists Conference*, Institute of Electrical and Electronics Engineers, Rhodes, Greece, pp. 2325–2328.

[59] MSC, 2017, “Bronze Spring Return Valve,” https://www.mscdirect.com/industrialtools/bronze-spring-return-valve.html

THIS PAGE INTENTIONALLY LEFT BLANK

INITIAL DISTRIBUTION LIST

1. Defense Technical Information Center
   Ft. Belvoir, Virginia

2. Dudley Knox Library
   Naval Postgraduate School
   Monterey, California